



## **1. Introduction**

A fighter plane had undergone problems during flight. The pilot observed excessive vibrations in the engine and landed the plane. The preliminary findings indicated problems in the turbine region. No foreign object damage (FOD) was observed. One 2nd stage turbine blade was found fractured. Other blades were found bent. To delineate the problem, components of the turbine region were examined and turbine blades of the 1st and 2nd stages were subjected to metallurgical investigation. Out of these the fractured blade (BF-11) was considered to be the cause of failure. The present study is the failure analysis of BF-11 turbine blade retrieved from the distressed engine. The findings are compared with other blades from the same engine and similar blades of other engines.

## **2. Hardware received for study**

Fifteen blades of the turbine region were received for study. The details of these blades and the purpose of study are summarized in Table 1.

### *2.1. History of the blades*

The engine has two stages of turbine blades. As mentioned in the literature provided, 2nd stage blades are fabricated from a creep resistant material. Working temperature in the turbine region gradually

Table 1

Blade no.	Stage	Condition	Purpose	Name <sup>a</sup>
11	2nd	Found fractured in service. Airfoil region missing	Received to confirm the mode and cause(s) of failure — the present study is focused on this blade	BF-11
21, 25, 40, 69, 53	1st	Retrieved from same engine and found in distressed condition	Included in the study as supporting evidence	BD-1s
10, 12, 20, 30, 40, 50	2nd			BD-2s
42	2nd	From another engine fracture seems similar to BF-11. Airfoil region missing	Studied as supporting evidence since the mode of failure is similar as that of BF-11	BF-42
20	1st	Normal blades retrieved after they have been in service, no abnormal defect	Included in the study for the purpose of comparison	BN-1s
38	2nd			BN-2s

<sup>a</sup> Nomenclature used in the present study.

decreases from 890 to 685°C from the 1st to the 2nd stage. Life of the blade is not specified but regular inspection is recommended. If the defects on the blades reach a given critical value, the blade is discarded. Blade BF-11 had completed a total of 892 h in service. The life of the other blades is not known. Regular overhauling of the engine is carried out. During overhauling visual, magnetic particle fluorescent inspection (MPFI) and dye penetrant inspection of the blades is performed.

Usually the blades are replaced due to defects caused by impacts, corrosion and cracks. The data of the rejected blades during the last 6 months are given in Table 2.

### 3. Fractured blades

The fractured blades BF-11 and BF-42 were subjected to detailed metallurgical examination. This includes visual examination, chemical analysis, microstructure, grain size measurement, hardness and fractography of the fractured surfaces. Chemical composition was determined with the help of energy dispersive spectrometry (EDS) and C/S analyzer. Samples were cut from different locations and prepared for optical and scanning electron microscopy. Etching was performed in gleceragia and then in 2% H<sub>2</sub>SO<sub>4</sub> in water. Grain size was measured using an image analyzer attached with the optical microscope. Hardness was measured by using Vicker's hardness testing machine. The fracture surfaces were examined with a scanning electron microscope (SEM). The scheme for the analysis of the blades is shown in the sketch in Fig. 1. The results are summarized in subsequent sections.

#### 3.1. Visual examination

The blade BF-11 had fractured from the region near the root area, see Fig. 2. The airfoil portion was not available. The fractured surface showed two clear regions (marked in Fig. 2) (i) a shiny region ~50% of the total fracture area and (ii) a dark black area covering the other 50% of the fractured surface.

Table 2

Defects	Impacts	Cracks	Corrosion
Blades rejected (%)	67	1	32

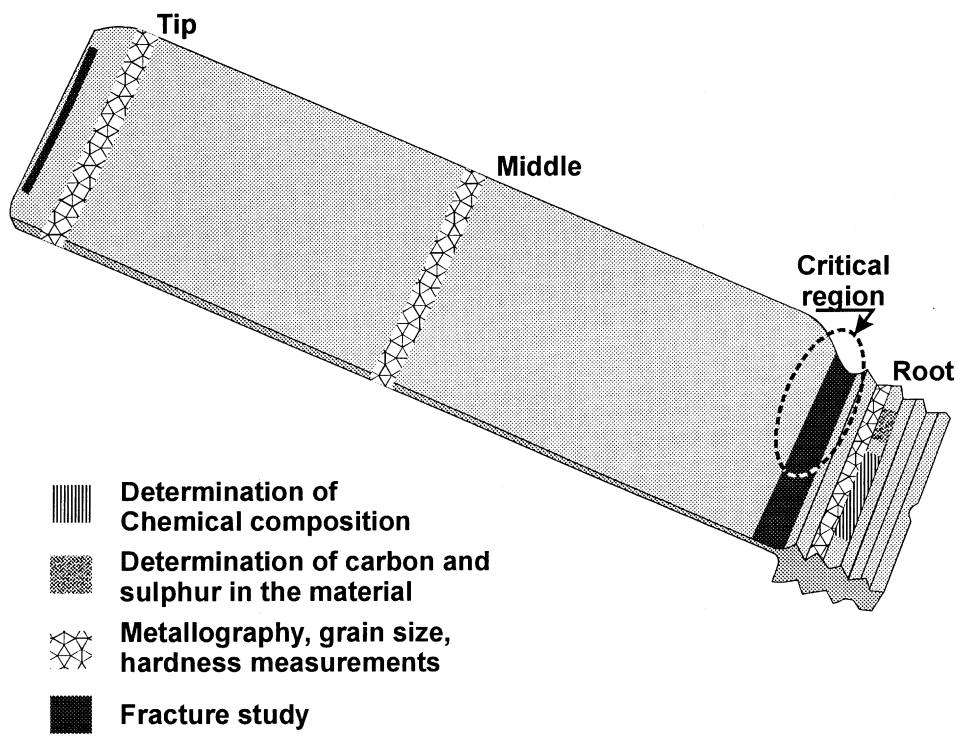


Fig. 1. Sketch showing the locations on the blade where different metallurgical tests were performed.

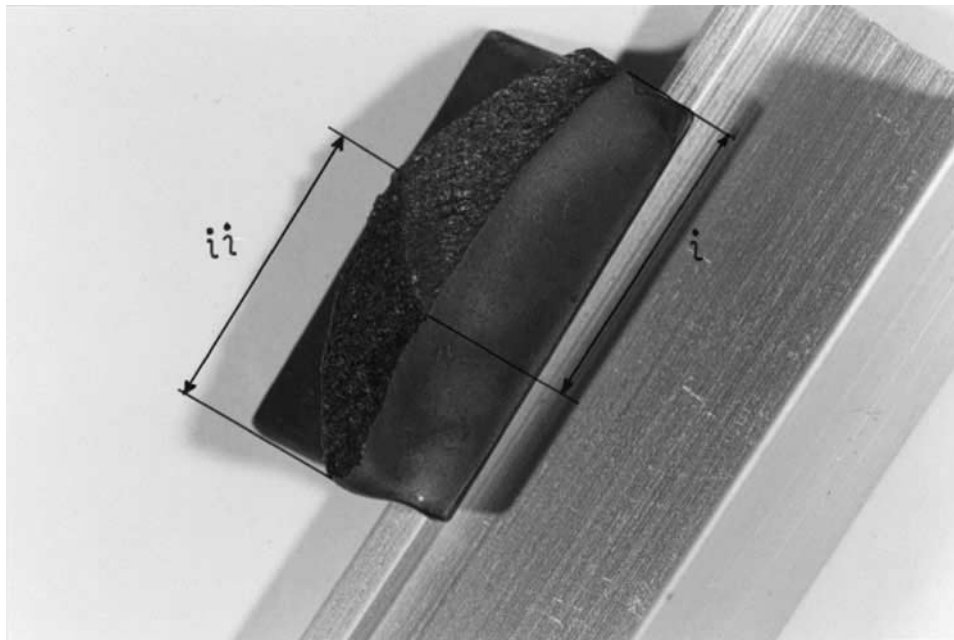


Fig. 2. Blade BF-11 fractured from the region near the root area.

Blade BF-42 also failed from the same location as BF-11. The airfoil region of this blade was also not found. The fracture surface showed similar fracture features as BF-11. The fracture surface showed a clear difference in colour in the different regions. Starting from the trailing edge a gradual change from light yellow to light blue to dark blue to dark brown and light brown was observed. The region, which finally ruptured, is dark grey.

### 3.2. Chemical composition

Chemical composition of the blades is given in Table 3. The closest standard material found in the literature is also given for comparison.

### 3.3. Microstructure

Specimens from fractured blades were cut and prepared for optical microscopy, see sketch in Fig. 1. In polished condition particles of yellow and grayish color are visible. EDS analysis shows high concentration of Ti and Mo in these particles. These are most probably carbides of Ti and Mo [1]. The carbides are mostly within grains and are coarse in size. However, fine carbides are also present along the grain boundaries. In longitudinal section these are aligned along the axis of the blades indicating that the blades are forged. The structure shows large grains, Fig. 3a. Inside grains slip bands are visible in most of the

Table 3

Element	Composition (wt.%)		Udimet 500
	BF-11	BF-42	
Cr	19.8±0.3	19.6±0.2	19
Co	18.1±0.5	18.4±0.4	19
Ti	3.5±0.3	3.2±0.2	3
Mo	3.1±0.2	3.6±0.1	3.6
Al	1.7±0.1	1.6±0.1	3
Fe	0.1	0.2	1 max
C	0.07	0.07	0.08
S	0.002	0.001	—
Ni	Bal	Bal	Bal

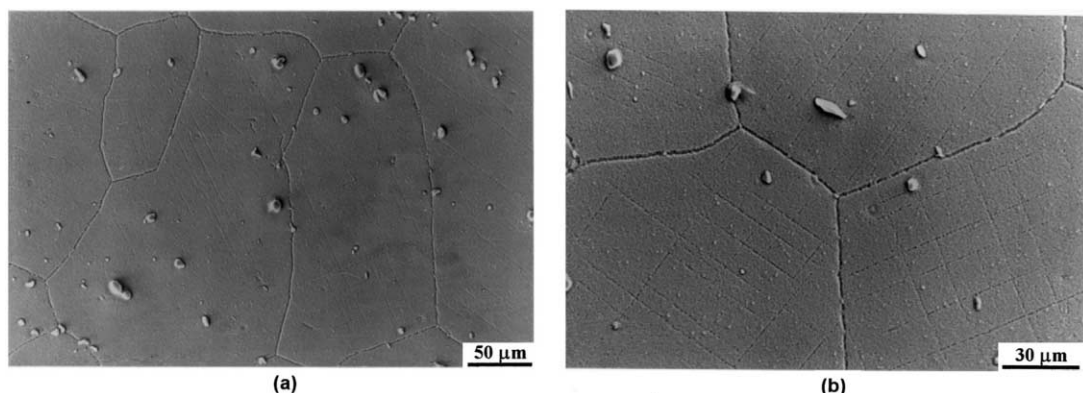


Fig. 3. (a) Large grain structure of the material; (b) slip bands inside grains appearing as fine parallel lines.

grains appearing as fine parallel lines, Fig. 3b. This is an indication that the part was under high stress. Twinning is also clear in some of the grains. Fine gamma prime, as expected in the material, is not resolvable at this magnification.

#### *3.4. Grain size*

Blade no.	BF-11	BF-42
Grain size ( $\mu\text{m}$ )	$145 \pm 66$	$162 \pm 85$

#### *3.5. Hardness*

Blade no.	Hardness (Hv)	
	BF-11	BF-42
Transverse section	$356 \pm 2$	$346 \pm 3$
Longitudinal section	$337 \pm 9$	$327 \pm 5$

#### *3.6. Fractography*

Fractured surfaces of the failed blades were examined in SEM. In blade BF-11 two regions are clear on the fracture surface at low magnification. The crack starts from the trailing edge on the airfoil next to the root region (Fig. 4a) (marked by arrow). This is the region where the cross-sectional area of the airfoil reduces before it joins the root of the blade. It is important to point out here that the cross-sectional area in this region is minimum and hence this region is bearing maximum stresses. Region II of the fatigue progression extends up to  $\sim 50\%$  of the fractured surface as is clear from Fig. 2. The crack started from the surface at location 'O' (Fig. 4b). An intergranular surface can be seen at this location at high magnification (Fig. 4c). In this region tear ridges are visible pointing back to the origin. Beach marks are also clear at the fractured surface before stage III starts (Fig. 5a). Coarse fatigue striations are clear at high magnification (Fig. 5b). After the fatigue crack reached a critical size the blade finally failed by an overload mechanism. In this stage (III) the fracture is predominantly intergranular (Fig. 6a). Secondary cracking showing triple point cracks is visible in the fracture area (Fig. 6b and c).

In the blade BF-42 the same features of fracture are present. The fatigue crack seems to start from surface cracks while multiple origins are present. Intergranular fracture is clear at the origins. Fig. 7 clearly shows that fine cracks (C) were present at the surface (S), which became the sites for fatigue crack (F).

### **4. Distressed blades**

Distressed blades were selected for metallurgical examination and subjected to same tests as fractured blades. The emphasis was given on the 2nd stage blades. However, the other blades were also examined as required.

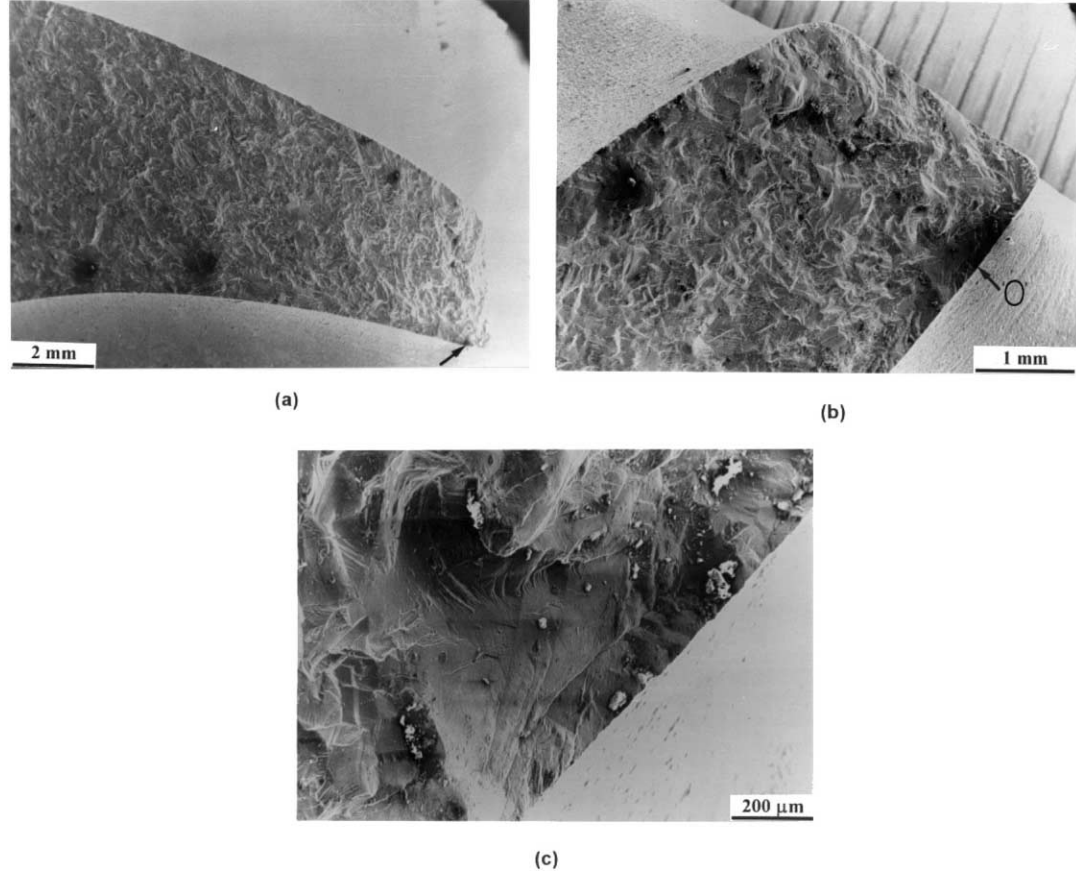


Fig. 4. SEM micrographs of the fractured surface: (a) arrow points to the origin; (b) high magnification showing the origin 'O'; (c) higher magnification of origin.

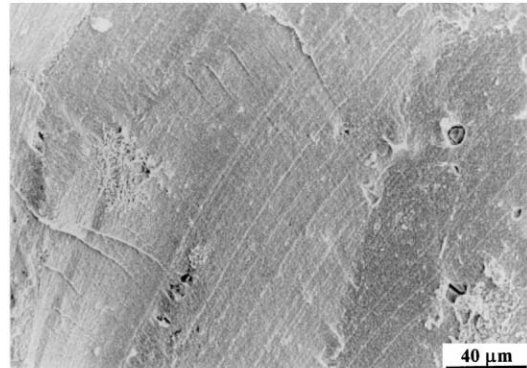
#### 4.1. Visual examination

##### 4.1.1. 1st Stage blades (BD-1s)

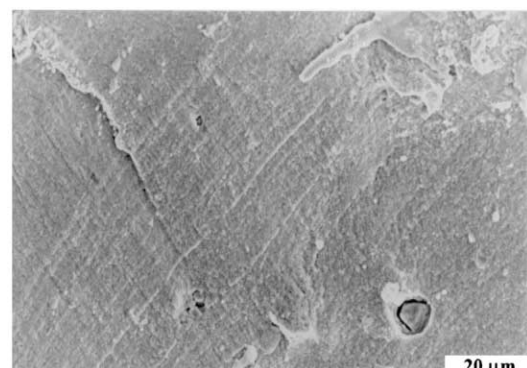
Visual examination of the BD-1s reveals that the tip of the blades is completely damaged (see Fig. 8a). The remaining area near the tip is bent from suction side to the pressure side. The blades have deformed in the airfoil region. This situation can arise when at high temperature different regions of the blades are subjected to mechanical impacts. Greenish deposits, most probably of Ni-Oxide, are present on the pressure side of the blades.

##### 4.1.2. 2nd Stage blades (BD-2s)

The 2nd stage blades also show erosion/corrosion in the tip region. However, the damage is greater on the leading edge as compared to the trailing edge (Fig. 8b). Deposits are also present on these blades mainly on the pressure side. Dents/scratches are present at isolated location on the surface of the blades, which reflect mechanical impact.



(a)



(b)

Fig. 5. (a) Beach marks at the fracture surface before stage III starts; (b) coarse fatigue striations at high magnification.

#### 4.2. Stereomicroscopy

The distressed blades were subjected to stereomicroscopy, up to a magnification of 50 $\times$ , to examine the surface defects.

##### 4.2.1. 1st Stage blades

Surface of the blades (BD-1s) was carefully scanned specially the area from where the crack started in the fractured blades. No cracks were revealed in this region of the blades. However, fine cracks, if present, can not be seen at this magnification (see Section 4.4). The eroded/fractured area near the tip shows intergranular fracture. It is quite possible that these regions experienced impact.

##### 4.2.2. 2nd Stage blades

Among 2nd stage blades, blade No. 10 (BD-210) shows extensive cracks on the surface, at the region from where the crack in blade BF-11 started. The cracks are extremely fine and barely appear at 100 $\times$  and are easily seen at high magnification. It looks as if the cracks were developed at the grain boundaries. The regions at the tip of the blade from where the material is removed also show intergranular fracture. Grains are clear at the fracture surface.

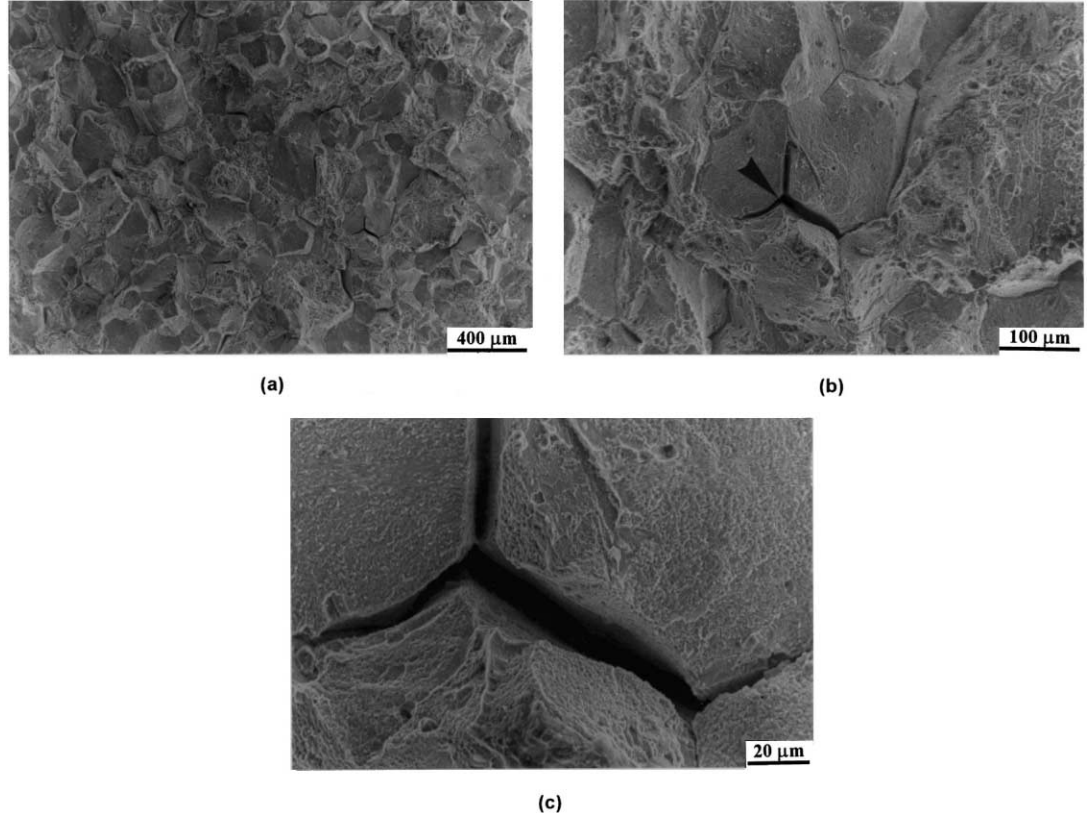


Fig. 6. (a) Predominantly intergranular fracture in stage (III); (b) secondary cracking showing triple point cracks — arrow; (c) high magnification.

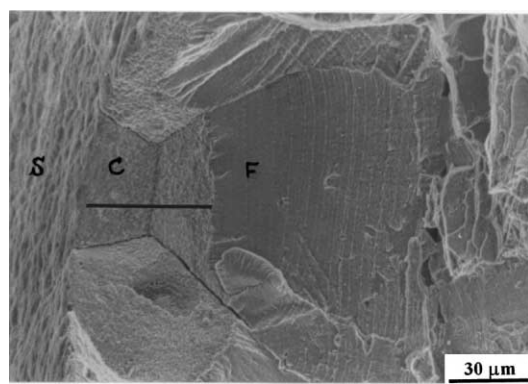


Fig. 7. Fine crack 'C' at the surface 'S' which became the site for fatigue crack 'F'.

#### 4.3. Non destructive testing

NDT was carried out on 2nd stage blades to reveal surface and internal cracks/ defects. Distressed blades Nos. BD-210, 212, 220, 230 and BN-238 were subjected to radiography and dye penetrant techniques.

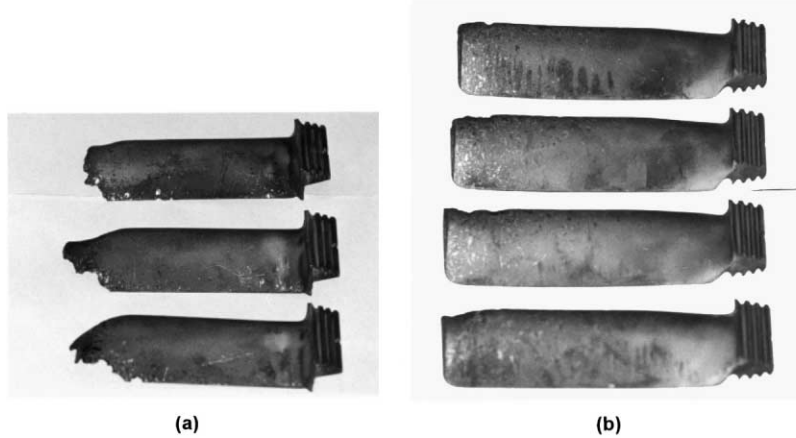


Fig. 8. Distressed blades; (a) 1st stage; (b) 2nd stage.

NDT techniques used could not resolve the cracks. The cracks found in the blade BD-210 were confirmed in cross-sectional view (see Section 4.7).

#### 4.4. Scanning electron microscopy

BD-210 was placed in SEM and the region where the cracks were found in stereomicroscopy was examined at high magnification (Fig. 9a) (critical region marked in Fig. 1). SEM examination confirmed that the cracks were present on the surface in that region. The cracks developed along the grain boundaries (Fig. 9b-d). This type of crack is referred as w-cracks or triple point cracks [2]. The chemical analysis of the surface showed presence of P and Ca in this region.

#### 4.5. Chemical composition

Chemical analysis of the distressed blades from 1st (BD-140) and 2nd (BD-210, 212) stages was carried out and the results are tabulated in Table 4.

#### 4.6. Hardness

Hardness of the blades was measured from different locations as shown in the sketch in Fig. 1. The results are given in Table 5. The results of hardness measurements show variation in different regions of the blades. High hardness is generally found in the regions near the damaged tip where the cracks on the surface are present and on the leading edge. In these regions, hardness values up to 430 Hv were found at some locations.

#### 4.7. Microstructure

The microstructure of distressed blades (BD-1s and BD-2s) shows the same features as found in the fractured blades. In the section taken from the blade BD-210, from the region of cracks, fine surface cracks were visible. The cracks run along the grain boundaries and their depth varies from 10 to 15  $\mu\text{m}$ . No oxidation was observed along these cracks. The tip region of the first stage blades shows oxidation on the surface and along the grain boundaries.

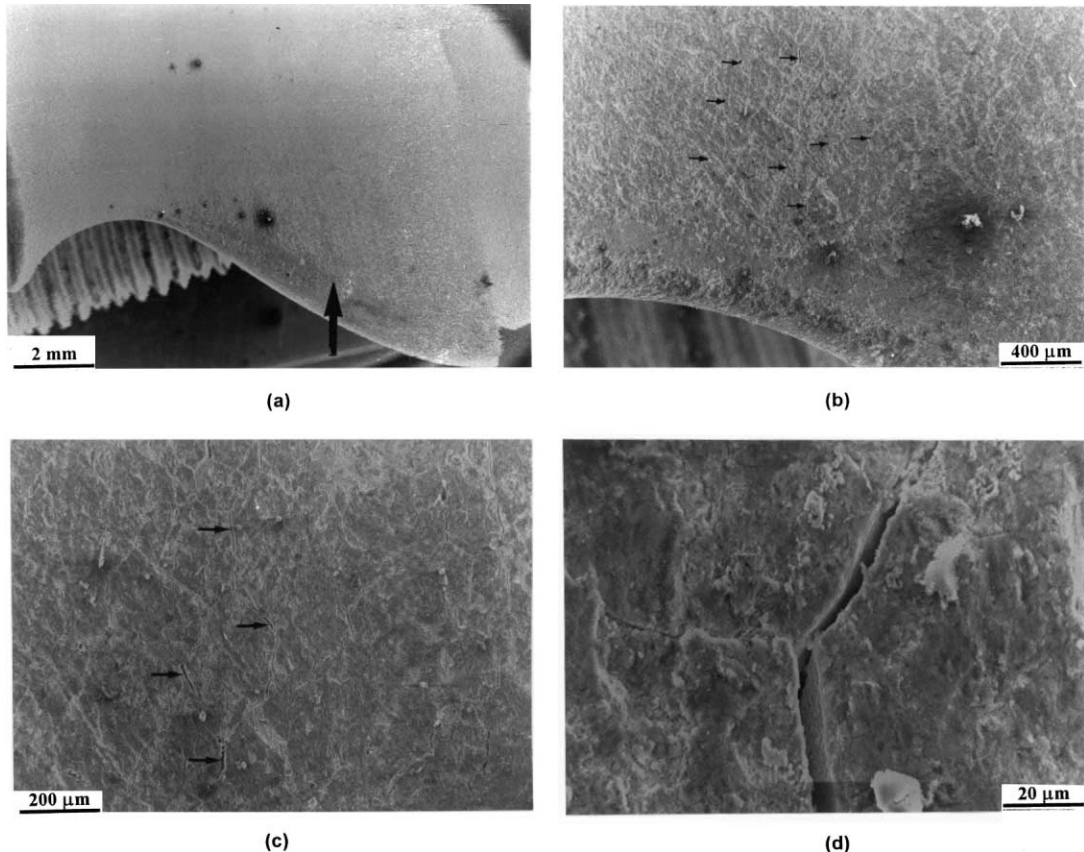


Fig. 9. SEM micrographs of blade BD-210: (a) location where cracks developed — ref. Fig. 1; (b) high density of the cracks; (c) cracks along the grain boundaries; (d) high magnification showing triple point cracks.

Blade BD-220 was cut, mounted and polished for metallography of the region near root area. In this blade no cracks were observed.

#### 4.8. Grain size

The results in Table 6 reveal that the average value of grain size varies in different blades as well as at different locations. However, the standard deviation from average value is also high, indicating that small and large size grains are present in the material.

### 5. Discussion

The results of chemical analysis indicate that the turbine blades of both the stages are manufactured from a Ni base super alloy. Ni base super alloys are used for applications where a combination of strength and hot corrosion is required at high temperatures. The alloy group is a precipitation-hardening and is heat treated to achieve required strength level to be used at high temperatures.

Two typical mechanisms of failure acting on the blades were creep and low cycle fatigue.

Table 4

Element	Composition (wt.%)		
	140	210	212
Cr	19.3±0.2	19.3±0.8	18.5±0.2
Co	18.6±0.1	18.2±0.0.2	18.7±0.4
Ti	3.7±0.2	3.5±0.3	3.1±0.2
Mo	3.3±0.1	3.6±0.1	3.1±0.1
Al	1.8±0.2	1.7±0.1	1.5±0.1
Fe	—	0.1	0.1
C	0.08	0.07	0.12
S	0.001	0.002	0.001
Ni	Bal	Bal	Bal

Table 5

Ref. Fig. 1	Hv
140R-root	359±4
210R	336±6
212R	368±5
210M-middle	342±4
212M	353±3
140T-tip	380±5
210T	372±8
212T	374±7

Table 6

Ref. Fig. 1	Grain size (µm)
140R-root	137±80
210R	195±124
212R	145±50
210M-middle	170±96
212M	106±70
140T-tip	115±64
210T	190±90
212T	180±115

### 5.1. Crack formation by grain boundary sliding (creep)

Metals and alloys when subjected to high temperature tests, the fracture path changes from transgranular to intergranular with increasing temperature [2]. Transgranular fracture occurs at low temperatures at which the slip planes are weaker than the grain boundaries. At high temperatures the grain boundaries are weaker and fracture is intergranular. Such observations have led to the introduction of the equicohesive temperature concept to define the temperature at which the grains and grain boundaries exhibit equal strength: that is the temperature at which the fracture mode changes from transgranular to intergranular. The equicohesive temperature is not a fixed temperature but varies with the stress and strain rate for a

given composition. Above the equicohesive temperature coarse-grain specimens exhibit greater strength than fine-grain specimens because of the lower grain-boundary surface area.

Tests at temperatures above the equicohesive temperature have revealed two types of intergranular fracture. When grain-boundary sliding occurs wedge-shaped cracks may form at grain-boundary triple points (as observed on a plane-of-polish) if the tensile stresses normal to the boundaries exceed the boundary cohesive strength. In the literature, these cracks are referred to as wedge or 'w-type' or as triple point or grain-corner cracks. High stresses promote this type of crack formation.

Under low-stress condition intergranular fractures occur by void formation at the grain boundaries. These cavities form along grain edges rather than at grain corners. Because they appear to be round or spherical on metallographic cross-sections these voids are sometimes referred to as r-type cavities. Inclusions and precipitates on grain boundaries can act as sites for void nucleation.

### 5.2. Low cycle fatigue

The large final overstress area shows that a system of low cycle fatigue (LCF) was operative on the blade. In the case of aircraft engine failure analysis LCF is considered to be related to mission or throttle [3].

The characteristics of LCF are (these are tendencies and may not be observed in all cases):

1. High cyclic stress
2. Driven by mission or throttle
3. Striations usually visible on SEM
4. Relatively insensitive to surface condition
5. Stress may be greater than yield
6. Propagation controlled
7. Large final over stress area
8. Small scatter in life

In the blades BF-11, BF-42 and BD-210 'w-cracks' were observed. These are typically found in a material which is exposed to high stress above *equicohesive* temperature. The photomicrograph in Fig. 9c very clearly indicates high stresses along the blade axis resulting in a high density of 'w-cracks'. The sliding of grain boundaries continued to generate initial cracks. In the blades studied, the subsequent propagation of cracks is controlled by cyclic stresses. The region that has undergone these two phenomena i.e. (i) grain boundary sliding and (ii) fatigue propagation is clearly visible in the photomicrograph in Fig. 7.

100501616

# Materials safety: article exercise

The investigation used the following methods: visual examination of the fractured and distressed blades, energy dispersive spectrometry and C/S analyzer, microstructure analysis with optical microscopy, harness measurement using Vicker's hardness testing machine, fractography using Scanning electron microscope. Analyses were done for blades of the same engine and blades from other engines. The initial observation showed no foreign object damage. One 2<sup>nd</sup> stage blade fractured, which was the cause of the failure and other blades were bent. Visual examination on distressed blades revealed that the blade tips were damaged, the areas near the tips were bent, and the airfoil regions were deshaped. Carbides, slip bands and twinning were found by microstructure analysis. There are also features of crack initiation, propagation and intergranular fracture.

The primary cause of failure was due to creep and low cycle fatigue. The blades operated at high temperatures and there was temperature declining from the 1<sup>st</sup> stage blades to 2<sup>nd</sup> stage blades. The combination of high temperatures, stress and creeping led to grain boundary sliding and w-cracks. Under the high cyclic stress, these w-crack initiation points propagated into longer cracks. These mechanisms led to the failure of the turbine blades. This also reveals the two main mechanisms of failure: low cycle fatigue and creep. Due to the operating conditions in high temperature and high stress, the fracture path was intergranular, resulting in the presence of w-cracks. Evidences for low cycle fatigue was supported by striations on scanning electron microscope and a large overstressed area. Plastic deformation, brittle fracture and environmental assisted failure can be ruled out since there was no evidence indicated from the report.

To prevent similar failures, the blades should be redesigned using more suitable materials to withstand high temperature and high stress conditions. The design standard needs to be more conservative in case the quality of materials is not up to expectation or unpredicted factors appear during operation.



## **1. Introduction**

Nickel based superalloys are widely used as gas turbine blade material. They suffer from microstructural instabilities and environmental damages. The microstructure of nickel based superalloy turbine blades is mostly designed on the basis of precipitation of  $\gamma'$  phase in the  $\gamma$  matrix. Creep properties of the alloy are believed to be related to the volume fraction ( $V_f$ ) of the dispersed  $\gamma'$  phase and modulus misfit between  $\gamma'/\gamma$ . There are also ultra fine  $\gamma'$  phase that precipitate during aging stage of heat treatment of these alloys. The dissolution temperature of ultra fine  $\gamma'$  phase has been shown to be the temperature of flow stress drop [1]. Creep life and ductility of the alloy considerably reduced when exposed to a high temperature during service [2,3]. It is partly due to micro structural changes such as changes in  $\gamma'$  phase, carbide particles alignment at grain boundaries and micro void formation in microstructure. But the effect of environmentally related damage mechanisms must be considered as well. Grain boundary oxidation and dynamic embrittlement are two important damage mechanisms in nickel based alloys [4–6]. Once grain boundaries are attacked by this mechanism, the situation changes from bulk dependent creep damage to localized time-cycle dependent creep damage in the notch root produced by grain boundaries oxidation.

## **2. Background**

Cobalt based 40 MW gas turbine blades were replaced by those made of IN-738LC. The cobalt based superalloy had a life span of 50,000 h before much damage. The new blades made of IN-738LC failed in service after only 1500 h. Fig. 1 shows the

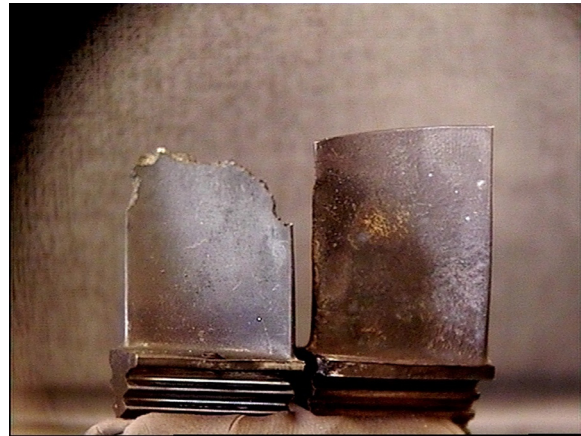


**Fig. 1.** Fractured blade and the intact one. The intact blade belongs to first series cobalt based blades that were replaced by IN-738LC.

Nickel based fractured blade and the intact one from first series of cobalt based blades which were chosen for materials evaluation.

### 3. Experimental technique

Chemical analysis of the blade was performed using optical emission spectrometer and EDS analyzer. Three transverse sections at root, mid height and top of airfoil beneath the fracture surface and one tangential section at the airfoil adjacent to fracture surface and one longitudinal section of the blade were prepared and electro etched for microstructural studies. Hardness of the blades had been measured in transverse and longitudinal sections. Fracture surface was studied using scanning electron microscopy TSCAN which was equipped with EDS analyzer.

### 4. Results

#### 4.1. Chemical composition

As shown in **Table 1**, chemical composition of the blade is the same as IN-738LC super alloy.

#### 4.2. Hardness test

Hardness test was performed on the blade according to ASTM E92 and E 384. Results of the hardness test are shown in **Table 2**. According to the test results, the hardness of the blade increases by moving toward the fracture surface up to 393 HV,

**Table 1**  
Chemical composition of failed blade.

Si	Cr	Mo	Co	Ti	Al	Nb	W
0.003	16.47	1.7	8.81	3.24	3.24	0.85	2.6 <sup>a</sup>
C	S	Zr	B	Ta	Al + Ti	Ni	
0.08	0.01	0.06	-	1.5 <sup>a</sup>	6.48	Base	

<sup>a</sup> Weight percent of W and Ta was measured by EDS analyzer.

**Table 2**  
Hardness test results of failed blade.

Test location	Vickers hardness (load 10 kgf) average of three points	Vickers micro hardness (load 50 grf) average of three points
Top of airfoil (transverse section)	393	-
Root (transverse section)	334	-
Mid height leading edge (transverse section)	348	407
Mid height trailing edge (transverse section)	358	435
Adjacent to fracture surface (longitudinal section)	-	447
Top of air foil (longitudinal section)	-	411
Mid height (longitudinal section)	-	373
Root (longitudinal section)	-	358
Adjacent to fracture surface (tangential section)	-	423

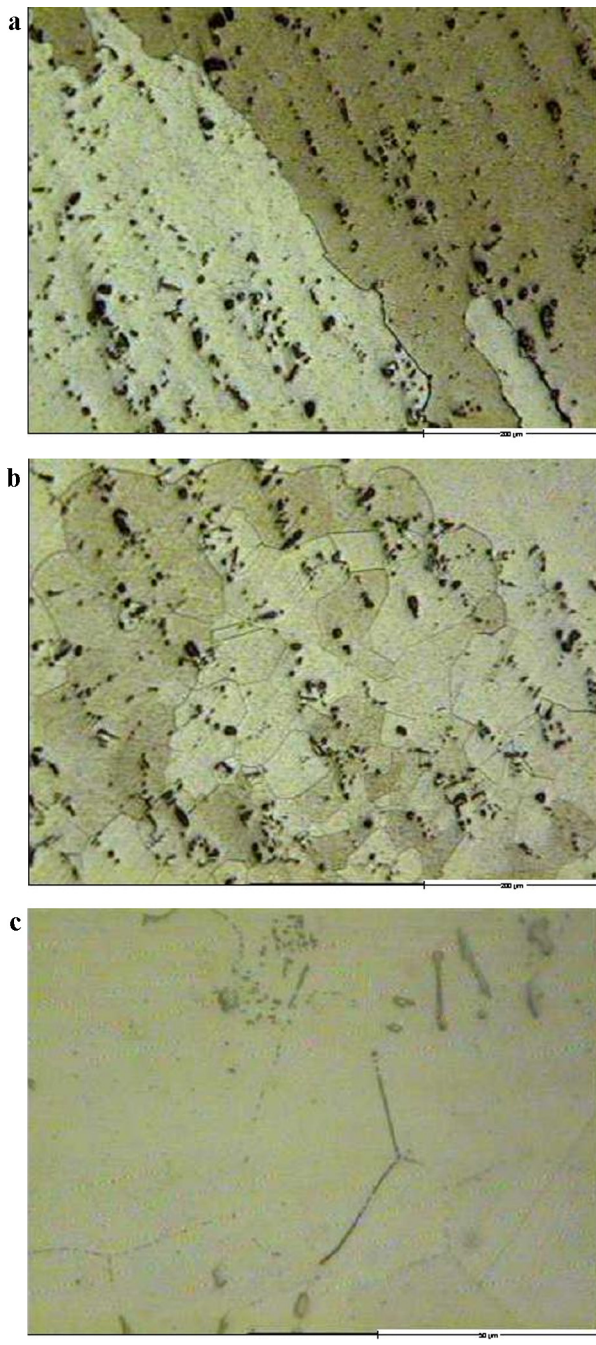


**Fig. 2.** (a) Macroscopic  $\gamma$  grains beneath the tangential section; (b) equiaxed fine  $\gamma$  grains at tangential section; and (c) fine precipitates at grain boundaries.

near to the fracture surface in comparison with mid height 350 HV and blade root 334 HV. This difference results from microstructural changes across the blade length.

#### 4.3. Microstructure

**Light microscopy:** Macroscopic  $\gamma$  grains are observed in different sections of blade (Fig. 2a), but there are some regions on tangential section that show fine equiaxed grains of  $\gamma$  with twinned areas (Fig. 2b). Grain boundaries in these regions are decorated by fine carbide precipitates (Fig. 2c).

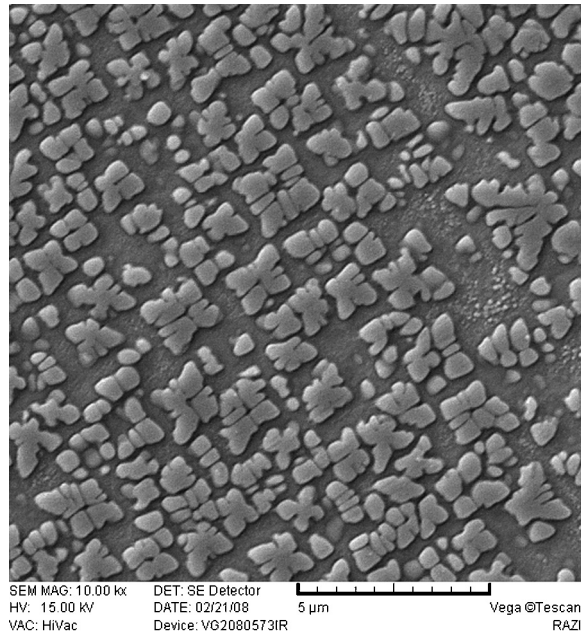


**Fig. 3.** Bimodal  $\gamma'$  in root of the blade.

**Scanning electron microscopy:** Microstructure of the root section of the blade is shown in Fig. 3 which consists of fine secondary  $\gamma'$  precipitates and clusters of cuboidal primary  $\gamma$  in  $\gamma$  matrix. Primary  $\gamma$  size in the root of blade was measured 190–760 nm.

After high temperature exposure, several aspects of microstructural changes occur in nickel base superalloys. Morphological changes including coarsening, rounding corners and agglomeration of  $\gamma'$  precipitates are more important aspects that are reported in literature [7].

The volume fraction of  $\gamma'$  is considerably reduced at the mid height section of the airfoil as shown in Fig. 4. Dissolution of primary  $\gamma'$  is obvious and secondary  $\gamma'$  particles could not be recognized in microstructure of the blade at this section. It seems that during service, fine secondary  $\gamma'$  particles dissolved into solid solution and dissolution of primary  $\gamma$  clusters took place as well.

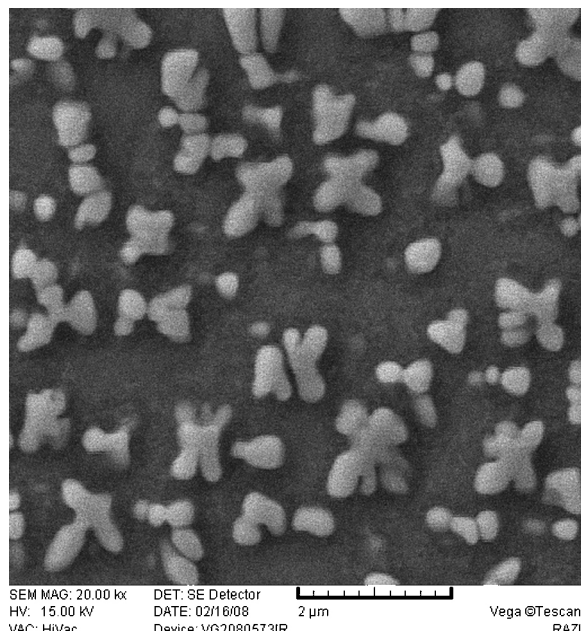


**Fig. 4.** Primary  $\gamma'$  dissolution in mid height of blade.

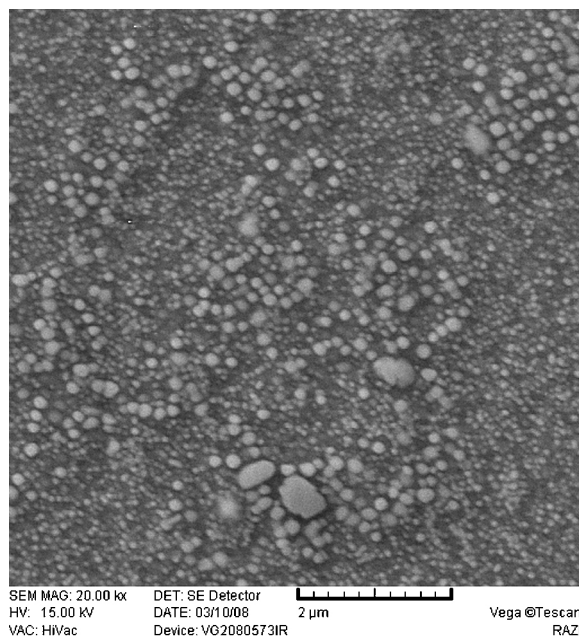
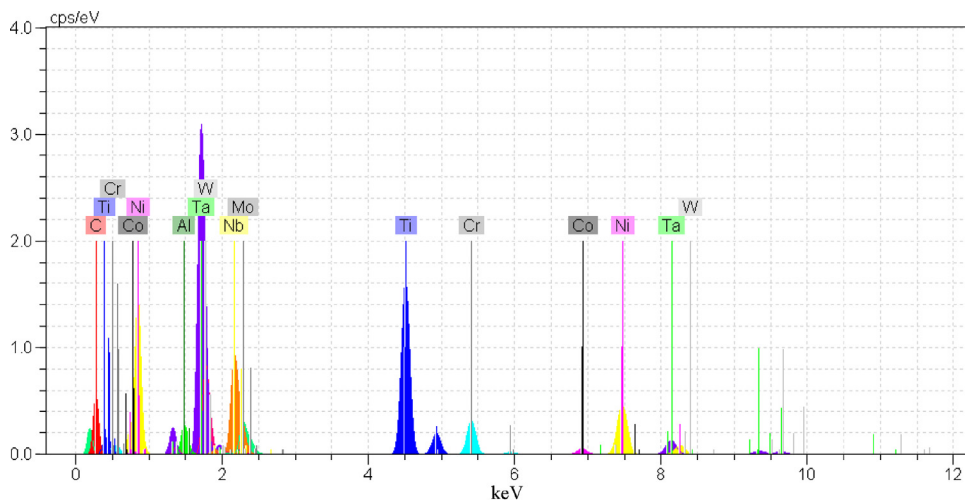


Fig. 5. Fine  $\gamma'$  precipitates in the tip of blade.

**Table 3**  
EDS analysis of MC carbide in root and tip of failed blade.



Element	Series	norm. C [wt.-%]	
		blade tip	blade root
Aluminum *	K series	1.3--1.7	-----
Titanium	K series	21.9--13.8	30.3
Chromium	K series	5.5--8.3	2.9
Cobalt *	K series	1.5--4.2	-----
Nickel *	K series	20.9--32.7	3.2
Niobium	L series	11--9.8	19.9
Molybdenum	L series	3.7--3.4	3
Tantalum	L series	16--17.5	29.7(Ta+W)
Tungsten	M series	7.9--5.5	-----

\*These elements are taken from base alloy analysis

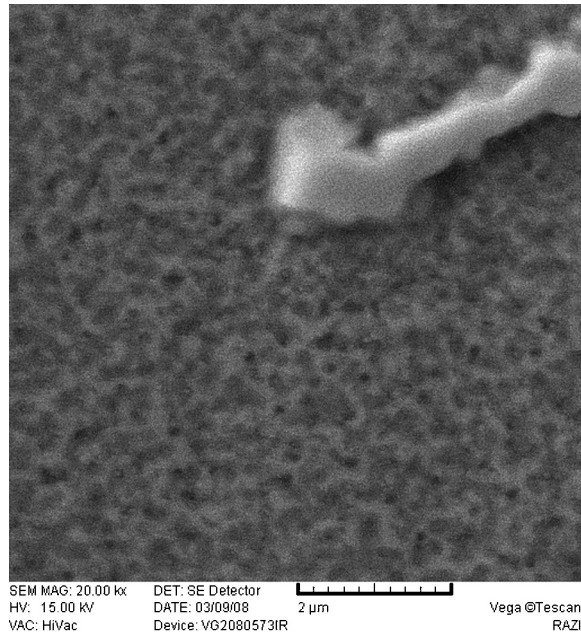


**Fig. 6.** Large MC carbide particle and fine dissociated  $M_{23}C_6$  particle.

In the tip of the blade there are some regions adjacent to the fracture surface that there are only a few remnants of primary  $\gamma'$  precipitates and extremely dense precipitates of secondary  $\gamma'$  are observed (Fig. 5). For this significant change in microstructure to happen it is required that the temperature of blade at the tip rise up to solution temperature of  $\gamma'$  [8].

The results of EDS analysis of MC carbides at root and tip of the blade are collected in Table 3. These results show that MC carbides in root of the blade are essentially based on (Ti, Nb, Ta, W and Mo) C. At the tip of blade, the chemical composition of MC carbides is more complicated.

According to these results, some of Ti and Nb are replaced by Cr and fine  $M_{23}C_6$  carbides formed around large MC particles (Fig. 6). Ni and Al are also involved in this process and it is obvious that in spite of the short life, the temperature at tip of blade was quite high for the reaction of  $\gamma + MC \rightarrow M_{23}C_6 + \gamma'$  to take place [9,10].

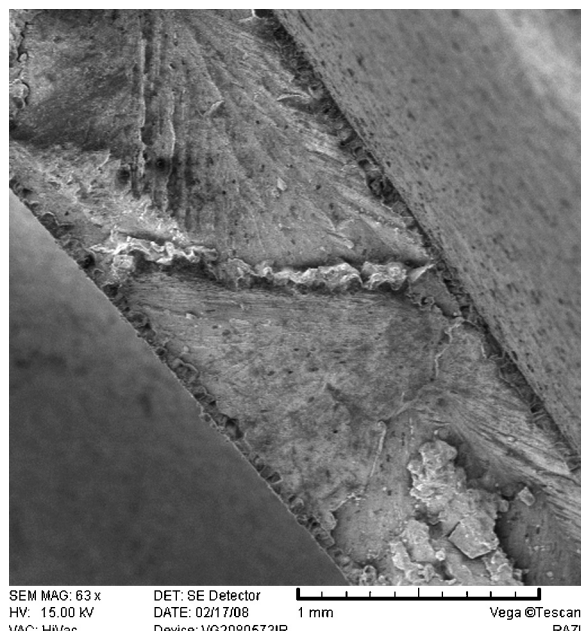


**Fig. 7.** A thin layer of intergranular fracture on perimeter of specimen.

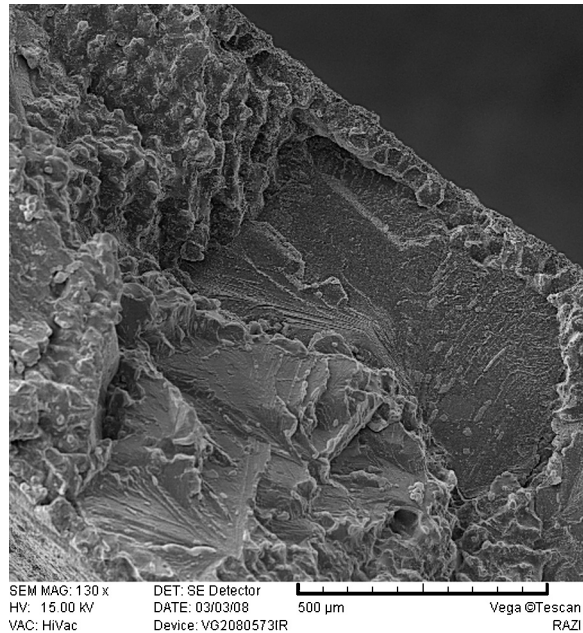


**Fig. 8.** Flat transgranular and interdendritic fracture.

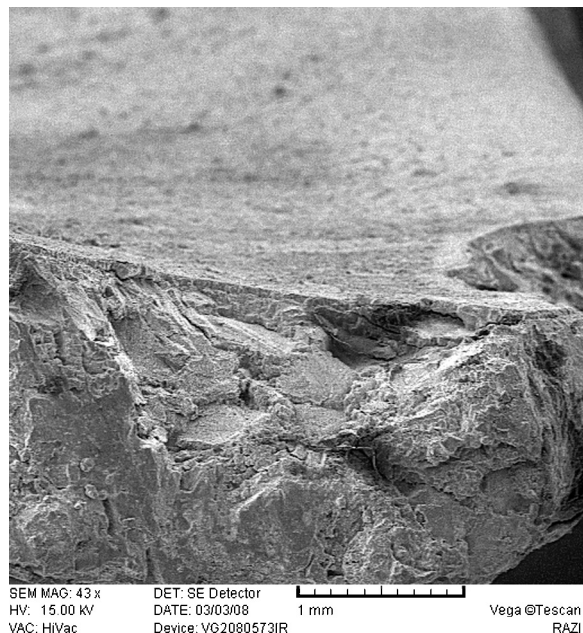


**Fig. 9.** Flat transgranular fracture in the leading edge of blade.

#### 4.4. Fractography

A thin layer of intergranular fracture about  $40 \mu\text{m}$  depths is observed on the perimeter of fracture surface (Fig. 7).

Flat transgranular is the feature of most fracture surface but there are also many regions in which interdendritic fracture could be seen (Fig. 8).

In the leading edge of blade the fracture is completely flat transgranular (Fig. 9).

**Fracture mechanism:** The thin brittle intergranular fracture layer on the perimeter of fracture surface is the results of three dimensional growths of the grain boundary cracks in fine grained area of the blade (Fig. 10). It is believed that stress assisted grain boundaries oxidation and restricted grain boundary sliding are the two dependent fracture mechanisms in this zone.

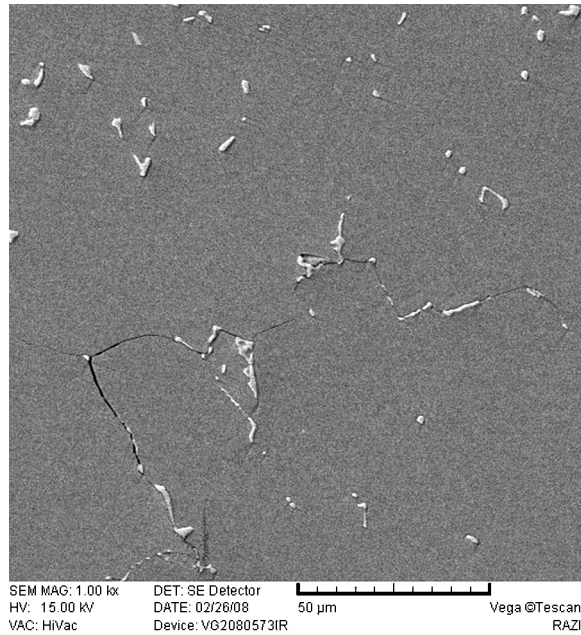


**Fig. 10.** Grain boundaries cracks at the surface of blade.

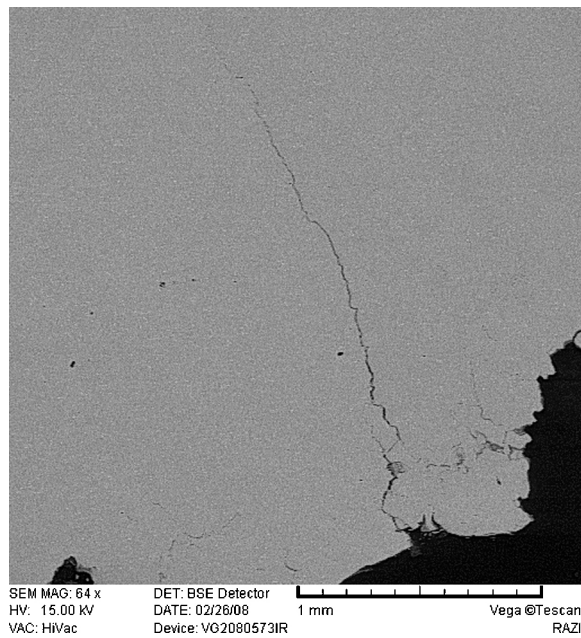


**Fig. 11.** Interdendritic growth of cracks on blade surface.

Below this layer cracks did not follow grain boundaries up anymore and developed in interdendritic carbide paths into blade thickness (**Fig. 11**).

Micro voids coalescence into wedge cracks at grain boundaries were observed in interdendritic regions on fractured surface (**Fig. 12**).

Incremental growth of crack in fracture surface shows that dynamic embrittlement plays an important part in fracture (**Fig. 13**).

Finally inside the large macroscopic grains, microstructural change because of high temperature exposure resulted in matrix planar slip and consequently flat crystallographic features appeared in fracture surface (**Fig. 14**).

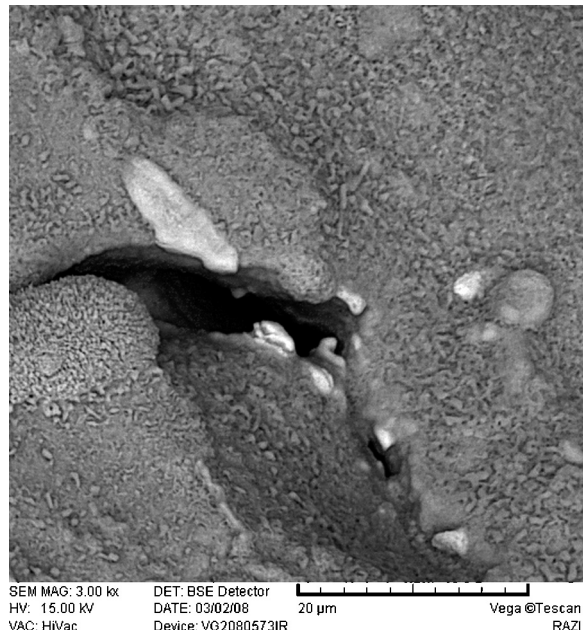


Fig. 12. Micro voids coalescence into wedge crack at grain boundaries on blade fracture surface.

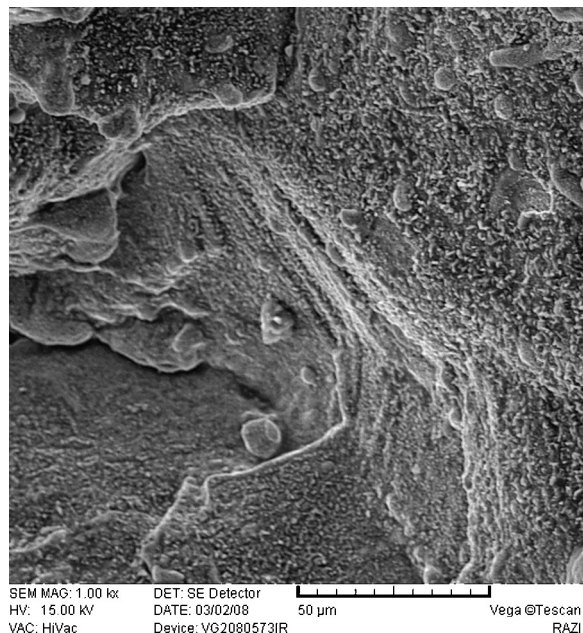


Fig. 13. Incremental crack growth in fracture surface.

## 5. Discussion

Grain boundary oxidation is the first mechanism that was easily recognized during microstructural studies of the blades. This mechanism is active when blades are exposed to a very high temperature. Shallow notches at airfoil surface converted to dip notches covered by oxidic layers and cracks developed intergranularly from these notches. Some of these oxidic cracks developed interdendritically.

The circumferential intergranular fracture layer divides the fracture surface into two zones. The first zone with the depth of 40 μm (equal to one  $\gamma$  grain width) at surface is a thin layer zone that the fracture surface is brittle and granular. Beyond this layer, there is a large zone that shows the activation of two independent fracture mechanisms. The first one with

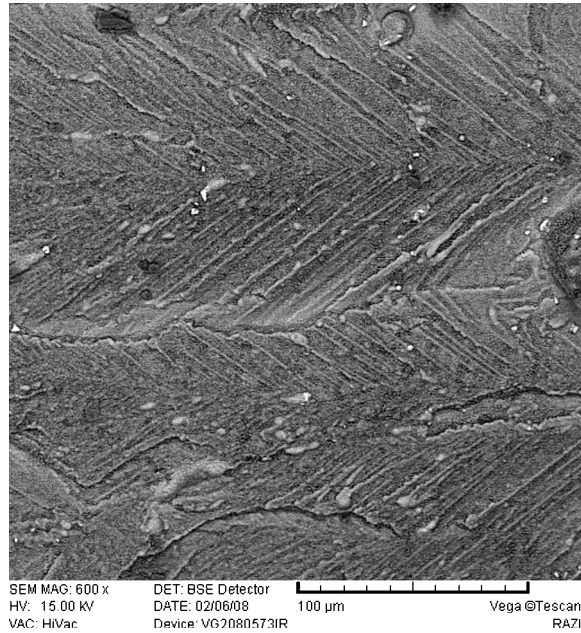


Fig. 14. Flat crystallographic fracture in large grains.

interdendritic–oxidic crack growth is due to stress assisted environmental damage [8] and bearing in mind the microstructural changes and ductility deterioration of blade due to high temperature exposure, the facilitated wedge crack formation according to classical creep damage mechanism could be explained in this region.

Flat transgranular crystallographic fracture regions that are observed in this zone shows that planar slip has occurred within large  $\gamma$  grains. Dissolution of  $\gamma'$  precipitates accelerates creep and decreases the ductility of the alloy in these regions.

493905

Markus Forsback 493905

### Nickel based superalloy as gas turbine blade material catastrophic failure report.

The failure report discusses the usage of nickel-based superalloy in a gas turbine blade material. Former cobalt based gas turbine blades were replaced by those made of IN-738LC material. According to the report, the failure of the new blades happened after about 1500 hours. This is vastly lower time than the old cobalt-based gas turbine blades which lasted 50,000 hours before showing signs of damage. Several means of investigation were used in the analysis of the failure. These include chemical composition analysis, hardness tests and microstructure analysis. Chemical composition was obtained by using an EDS (Energy-dispersive X-ray spectroscopy) analyzer and optical emission spectrometer. The chemical composition of the gas turbine blade according to the analyzer is similar of that IN-738LC material. Although, there are usually small differences in the composition depending on the material manufacturer. Hardness tests were obtained by using ASTM E92 and E 384 standard. Although, the environmental conditions in which the hardness tests were obtained are not described in the analysis. Only the results of hardness tests are shown. The hardness tests show that the closer the tests are taken from the fracture surface, the harder the material is. The analysis provides a reason for this as it mentions that there are changes in the microstructure of the material across the blade. Microstructure was analyzed by scanning electron microscopy and. Several fractography figures of the surface of the blades were obtained by using the microscopy. These figures are represented in the analysis and provide information about the nature of the fracture.

There were two failure mechanisms observed in the analysis. The primary one discussed was grain boundary oxidation, which can happen to IN-738LC in high temperatures. And the secondary one was stress assisted environmental damage such as creep. Both can happen simultaneously in the material. Grain boundary oxidation was deemed as one of the failure mechanisms as there were several changes in the microstructure that suggested that grain boundary oxidation happened. These include the dissolution of gamma precipitates in the material surface. Generally, gamma precipitates are solid particles that are dispersed throughout the material, providing increased strength to the material. These can be further categorized as secondary and primary precipitates. However, based on the analysis, primary gamma precipitates were absent in some regions of the fracture surface and only large amounts of secondary precipitates were prevalent. This would suggest that high temperature has caused dissolution of some of the primary precipitates. Therefore, weakened the structural integrity of the blades. Another reason for grain boundary oxidation would be the mechanism of which the fracture happened. According to the analysis the fracture was intergranular for a brief period. Until it became transgranular in the leading edge of the blade. This further increases the odds that oxidation happened at the surface of the blade fracture. Transgranular fracture is a strong sign of brittle material. It is possible that the material surface of the blade had been corroded to become brittle. Also, in figure 13 incremental crack growth can be seen in fracture surface which is also a strong sign of brittle fracture. The secondary cause for failure according to the analysis was creep damage. Micro voids and cracks in the material surface were observed in the fractographic figures which would be a strong indication of creep damage.

According to the analysis the chain of action that led to the failure was caused by the combination of creep damage and oxidation of the grain boundaries in high temperatures. IN-738LC is susceptible to oxidation of grain boundaries in high temperatures. Oxidation causes the diffusion of oxygen in the grain boundaries. The blades were operated in high temperatures and the oxidation of the grain boundaries happened. Leading to embrittlement of the material. In addition to oxidation, creep damage started to form in the material which caused fractures in the material surface and diffusion of

atoms. These effects combined caused the gamma precipitates to dissolve and the structural integrity of the material was weakened substantially leading to a catastrophic failure during operation.

Based on the figures and information provided in the report, plastic deformation cannot be ruled out. There are dimple patterns seen in figure 8. Which are commonly found in fractures caused by plastic deformation. There are also very few figures about the crack growth in the blade edge which makes it hard to determine how exactly the fracture happened. Also, there is no information provided about the possible loads happening to the blade. Although, plastic deformation is a very unlikely event in gas turbine blades, it still cannot be ruled out based on the information given in the report. With more details provided, plastic deformation could probably be ruled out.

Creep cannot be ruled out either. There are very strong indications about creep happening in the blade mentioned in the chapters above and it is one of the more likely failure mechanisms that happened.

Brittle fracture cannot be ruled out. Some of the fractographies like figure 8. show brittle like features such as transgranular fracture surface and beachmarks. These are commonly regarded as brittle fracture features. It is likely, that brittle fracture happened.

Fatigue cannot be ruled out. There is no mention about the load cycles that the material undergoes during operation. Fatigue can be seen as oxidation or corrosion of the fracture surface which closely resembles the information provided in the report. The results in the report very strongly indicate that fatigue may have had a hand in the failure. Although, it is not specifically discussed in the report.

Environmentally assisted failure cannot be ruled out. The blades operate in high temperatures and are susceptible to gas during operation. As the report mentions, this can cause oxidation. High temperature can cause structural damage to the atomic structure of the material. Environmentally assisted failure was the focus and the most likely failure mechanism discussed in the report.

Preventing creep or environmentally assisted damage is often hard. However, several methods can be applied to make it more unlikely. During material selection better material can be selected. IN-738LC material is suited for creep and good oxidation protection but it is susceptible to high cycle fatigue in high temperatures. Better protection from fatigue could be beneficial. Temperature can be monitored more closely which can reduce the chance for environmental damage to happen. Methods such as thermal insulation and cooling systems should be used to minimize the risks for creep. IN-738LC is susceptible to micro-cracking and strain age cracking during heat treatment. Proper heat treatment can reduce the risk for these to happen. Coatings can also be applied to the material which can slow down creep damage and protect from oxidation and corrosion. Providing higher probability for longer life cycle. Computational models can be employed to show possible failure signs before catastrophic failure happens.

602990

# Materials safety: article exercise

Nickel-based superalloys are commonly used in gas turbine blades, but they are susceptible to microstructural instabilities and environmental damage. The alloy's creep life and ductility are significantly reduced when exposed to high temperatures during service due to microstructural changes such as alterations in g0 phase, alignment of carbide particles at grain boundaries, and microvoid formation. Furthermore, environmentally related damage mechanisms like grain boundary oxidation and dynamic embrittlement can have detrimental effects on nickel-based alloys.

Previously, cobalt-based 40 MW gas turbine blades had a lifespan of 50,000 hours before experiencing significant damage. However, these blades were replaced with ones made of IN-738LC, which failed in service after only 1500 hours.

The investigation into the failure of gas turbine blades made of IN-738LC primarily utilized the following methods:

1. Chemical Analysis: The blade's chemical composition was analyzed using an optical emission spectrometer and EDS analyzer.
2. Microstructural Analysis: Transverse sections at various points on the blade, including the root, mid-height, and top of the airfoil, were prepared and electro-etched for microstructural studies using light microscopy and scanning electron microscopy (SEM).
3. Hardness Testing: Hardness tests were conducted at different locations on the blade, including transverse and longitudinal sections, using Vickers hardness measurements.

The primary cause of the failure of the IN-738LC gas turbine blades was identified as a combination of microstructural changes and environmental damage mechanisms, specifically grain boundary oxidation and dynamic embrittlement. The failure mechanism can be described as follows:

1. Microstructural Changes: Over time and exposure to high temperatures during service, several microstructural changes occurred, including:
  - o Dissolution of primary g<sub>0</sub> phase clusters.
  - o Reduction in the volume fraction of g<sub>0</sub> phase, especially at the mid-height section of the airfoil.
  - o Formation of fine equiaxed grains of g with twinned areas in certain regions.
2. Environmental Damage Mechanisms:
  - o Grain Boundary Oxidation: This mechanism becomes active at very high temperatures, leading to shallow notches at the airfoil's surface converting to deep notches covered by oxidic layers. Cracks developed intergranularly from these notches.
  - o Dynamic Embrittlement: Microvoids coalesced into wedge cracks at grain boundaries in interdendritic regions. Incremental crack growth due to dynamic embrittlement was observed.
3. Creep Damage Mechanism: The dissolution of g<sub>0</sub> precipitates accelerated creep and decreased the ductility of the alloy, especially in regions where flat transgranular crystallographic features appeared within large grains.

Based on the provided information and current knowledge, we can rule out certain alternate failure mechanisms:

- Plastic Deformation: While microstructural changes occurred, there is no evidence to suggest significant plastic deformation as the primary cause of failure.
- Creep: Creep is indeed a factor in the failure due to the dissolution of g<sub>0</sub> phase, but it is not the primary cause of failure.
- Brittle Fracture: The failure mechanism involved intergranular and interdendritic crack growth, but it is not characteristic of typical brittle fracture. It is primarily related to grain boundary oxidation and dynamic embrittlement.
- Fatigue: The failure mechanism does not exhibit fatigue characteristics but is attributed to environmental damage and microstructural changes over time.
- Environmentally Assisted Failure: The failure analysis clearly indicates the involvement of environmentally related damage mechanisms, such as grain boundary oxidation and dynamic embrittlement. Therefore, environmentally assisted failure is a significant factor in this case.

To prevent similar failures in the future, several recommendations can be made:

1. Microstructure Control: Ensure strict control over the microstructure of the alloy, particularly the volume fraction and stability of g<sub>0</sub> phase. This can be achieved through precise heat treatment processes and material composition adjustments.
2. Temperature Monitoring: Implement continuous temperature monitoring of the gas turbine blades during operation to detect and manage high-temperature exposure.
3. Materials Research: Invest in research to develop alloys with improved resistance to grain boundary oxidation and dynamic embrittlement.



4. Regular Inspection: Establish a regular inspection and maintenance schedule to detect early signs of microstructural changes and damage mechanisms.
5. Improved Design: Consider blade design modifications that reduce stress concentrations and minimize the impact of environmental factors on the blade's integrity.

100509058

## 1 Introduction

In today's era, nickel-based superalloys have become a prevalent choice for the primary material in turbine blade construction. The unique microstructure of these superalloys makes them particularly sensitive to elevated temperatures, significantly influencing their resistance to creep and ductility. Besides alterations in microstructure at high temperatures, phenomena such as grain boundary oxidation and dynamic embrittlement also contribute to changes in material behavior under such conditions. These mechanisms are categorized as environmentally induced damage mechanisms. This report summarizes an in-depth study of why turbine blades made of IN-738LC failed. These blades were originally made of cobalt-based superalloys and ran for 50,000 hours without issues. However, the new nickel-based blades failed after just 1,500 hours.

## 2 Investigation Methods

Chemical analysis of the blades was conducted using both an optical emission spectrometer and an EDS analyzer. A total of five sections were prepared for microstructural analysis, consisting of three transverse sections, one tangential section, and an additional tangential section. The transverse sections were strategically selected at the root, mid-height, and just below the fracture surface of the blade, while the tangential section was chosen from the airfoil region adjacent to the fracture surface. Furthermore, several additional sections underwent hardness testing. Lastly, the fracture surface was subjected to analysis using a scanning electron microscope.

## 3 Results

The chemical analysis successfully identified the blade material as IN-738LC. Hardness tests were conducted following ASTM E92 and E 384 standards, and the results indicated a gradual increase in hardness as one approached the fracture surface, peaking at 393 HV at the top of the airfoil. This variation in hardness was attributed to microstructural alterations that occurred along the length of the blade.

The blade's macroscopic observation reveals the presence of  $\gamma$  grains in various sections, with certain regions on the tangential section displaying fine equiaxed grains of  $\gamma$  with twinned areas. These regions exhibit grain boundaries adorned with fine carbide precipitates. The microstructure of the root section showcases fine secondary  $\gamma'$  precipitates alongside clusters of cuboidal primaries  $\gamma'$  within the  $\gamma$  matrix, with primary  $\gamma'$  sizes ranging from 190 to 760 nm.

After exposure to high temperatures, notable microstructural changes occur in nickel-based superalloys, including morphological alterations such as coarsening, rounding of corners, and agglomeration of  $\gamma'$  precipitates. The volume fraction of  $\gamma'$  significantly diminishes in the mid-height section of the airfoil, with the dissolution of primary  $\gamma'$  being evident, and secondary  $\gamma'$  particles no longer recognizable in the blade's microstructure at this section. At the blade's tip, there are regions adjacent to the fracture surface where only a few remnants of primary  $\gamma'$  precipitates remain, alongside extremely dense precipitates of secondary  $\gamma'$ . This dramatic microstructural change suggests that the blade's tip reached the solution temperature of  $\gamma'$ .

Furthermore, the EDS analysis of MC carbides at the root and tip of the blade reveals differences in chemical composition.

The fracture analysis reveals a thin intergranular fracture layer around the perimeter, along with some interdendritic regions. The primary fracture mechanisms include stress-assisted grain boundary oxidation and constrained grain boundary sliding, leading to the intergranular layer. Below this layer, cracks transition to interdendritic carbide paths. Microvoids coalesce into wedge cracks, and dynamic embrittlement plays a role in crack growth. High-temperature exposure causes microstructural changes within large grains, resulting in flat crystallographic features on the fracture surface.

#### 4 Conclusion

During blade microstructural analysis, grain boundary oxidation was evident at high temperatures. Shallow notches on the airfoil surface transformed into dip notches covered by oxide layers, giving rise to intergranular cracks, with some appearing interdendritically.

A circumferential intergranular fracture layer divided the surface into two zones. The first, extending 40 mm deep from the surface, displayed a brittle, granular texture. Beyond this layer, two fracture mechanisms emerged: interdendritic-oxidic crack growth due to stress-assisted environmental damage and facilitated wedge crack formation consistent with classical creep damage mechanisms.

Flat transgranular crystallographic fracture regions within this zone indicated planar slip within large  $\gamma$  grains, while the dissolution of  $\gamma'$  precipitates accelerated creep and reduced alloy ductility.



## 1. Background information and service history

Metallic assemblies exhibit lower service-life when operated at elevated temperatures. Depending on the particular environmental and loading conditions, the most common causes of elevated-temperature failure can be classified as creep-originated, environmentally induced, high-temperature fatigue and thermal fatigue [1].

The present study focuses on the investigation of the systematic short-time failure of a superheater pipeline, part of the main heat exchanger assembly operating with steam, in a power-plant unit in Northern Greece. The multi-curved pipeline was constructed over a lignite combustor, 30 years ago. According to the original design, the whole pipeline consists of an array of individual tubes of outer diameter 38 mm, wall thickness 6 mm and length 4 m. These tubes are properly welded to form a pipeline with a total heat exchange area of 5200 m<sup>2</sup>. The suggested construction materials were the steel grades: 15Mo3, 13MoCr44 and 10CrMo910 (Table 1), commonly proposed for the production of pressure vessels.

The average steam velocity along the pipeline was 9.1 m s<sup>-1</sup> and the steam outlet flow rate 893 t h<sup>-1</sup>. The operating conditions of the pipeline are summarised in Table 2.

An increased need for maintenance operations has been observed over the past several years, reaching eventually an average time period of 15 days of continuous operation. Such a high frequency introduces a costly procedure for the plant operation due to the plant downtime required for the repair/replacement of the failed pipeline parts. In the particular case, all the main elevated-temperature failure mechanisms are equally possible:

- Creep, due to the deviation between the designed and the actual operating conditions (abnormal operation).
- Environmentally induced failure, due to the effect of the combustion gases, the chemical composition of which can be diversified according to the lignite's mineralogical structure that can be crucially varied with the depth of the exploitation field.

**Table 1**

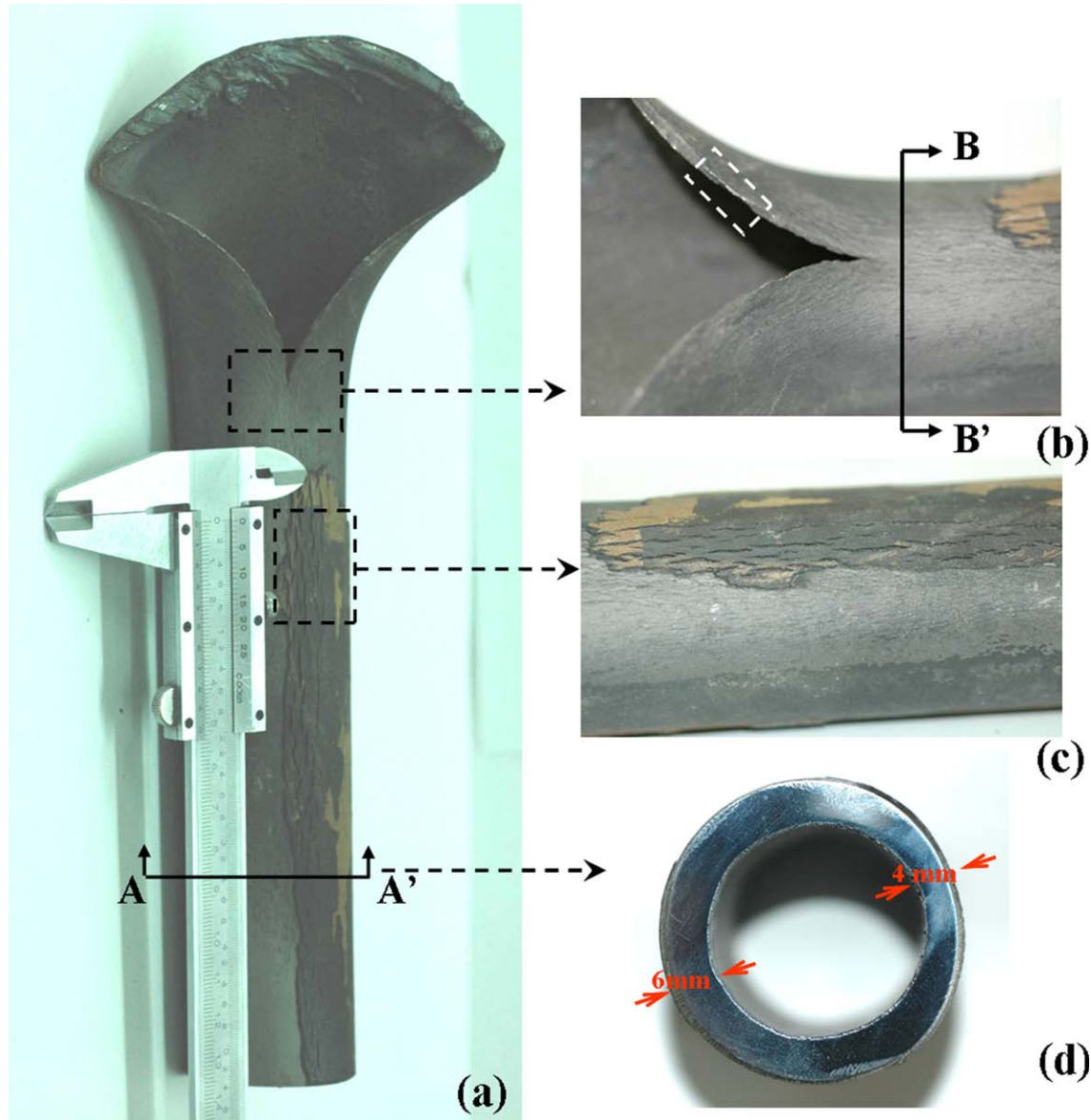
Chemical composition of the suggested steel grades (wt%)

Steel grade	W.Nr.	C	Si	Mn	P (max)	S (max)	Cr	Mo
15Mo3	1.5415	0.12–0.20	0.10–0.35	0.40–0.90	0.035	0.030	–	0.25–0.35
13CrMo44	1.7335	0.08–0.18	0.10–0.35	0.40–1.00	0.035	0.030	0.70–1.10	0.40–0.60
10CrMo910	1.7380	0.06–0.15	≤0.50	0.40–0.70	0.035	0.030	2.00–2.50	0.90–1.10

**Table 2**

Designed and actual operating conditions of superheater pipeline

	Designed	Actual
Steam inlet temperature (°C)	370	449
Steam outlet temperature (°C)	443	505
Steam inlet pressure (bar)	186.7	–
Steam outlet pressure (bar)	183.2	–

**Fig. 1.** Macrographs of the failed-tube retrieved from a curved area of the pipeline: (a) total view of the retrieved part, indicating "fish-mouth" rupture; (b) zooming of (a), at the area of the tip of the rupture lip; (c) zooming of (b), at the area of tube swelling and (d) cross-section ring along the line AA' of (a).

- Thermal fatigue, due to the frequent operation interruptions for the repair of the pipeline.
- High-temperature fatigue, due to alternations of the steam pressure.

The present study is focused on a thorough metallurgical investigation of the pipeline failed parts to identify the failure mechanisms and propose a more reliable solution, leading to maximum extension of the pipeline's service-life.

## 2. Experimental techniques

Macroscopic observations of the failed tubes were performed with a Leica MS 5 and a Nikon SMZ 1500 stereomicroscope. In order to reveal the main failure mechanisms, microscopic observations were carried out using an FEI XL40 SFE scanning electron microscope (SEM) equipped with an electron dispersive spectrometry X-ray microanalysis system (EDAX) for elemental analysis of selected areas. Metallographic examination was conducted using a Nikon Epiphot 300 inverted metallurgical microscope. Prior to that, cross-sections of the failed tubes were prepared using hot-mounting, wet grinding up to 1200 grit SiC paper and polishing with diamond and silica suspensions. Chemical etching was performed by immersion of the specimens in Nital reagent: 2% HNO<sub>3</sub> ethanol solution for 10 s, followed by cleaning with ethanol and drying with hot-air stream. Vickers hardness measurements on characteristic areas of the welded specimens were carried out using an Instron-Wolpert tester, applying a load of 10 kg [2].

## 3. Results

Systematic recording of data over one year of pipeline's service indicated that local material's failures were occurring with an average period of 15 days and were localised either at curved areas of the tubes, or in the neighbourhood of circumferential weldments. Microstructural investigations of failed-tube parts, representative of these two failure cases are discussed below.

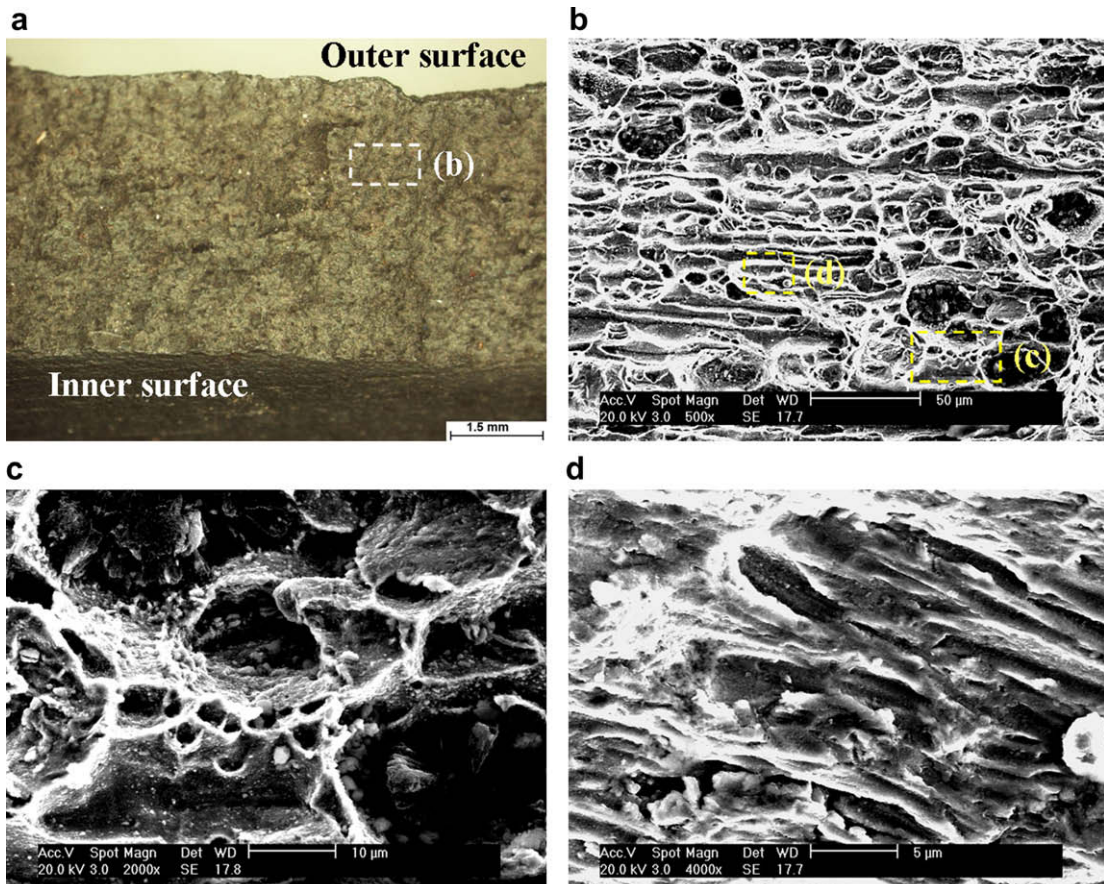


**Fig. 2.** Fracture surface of the rupture lips, indicated in Fig. 1a with a dashed rectangle: (a) stereo-graph of the dimpled fracture surface; (b) SEM image of the zoomed area indicated in (a); (c) SEM image of micro-voids, present on the fracture surface and (d) SEM image of dimples oriented along the initial direction of the material's grains.

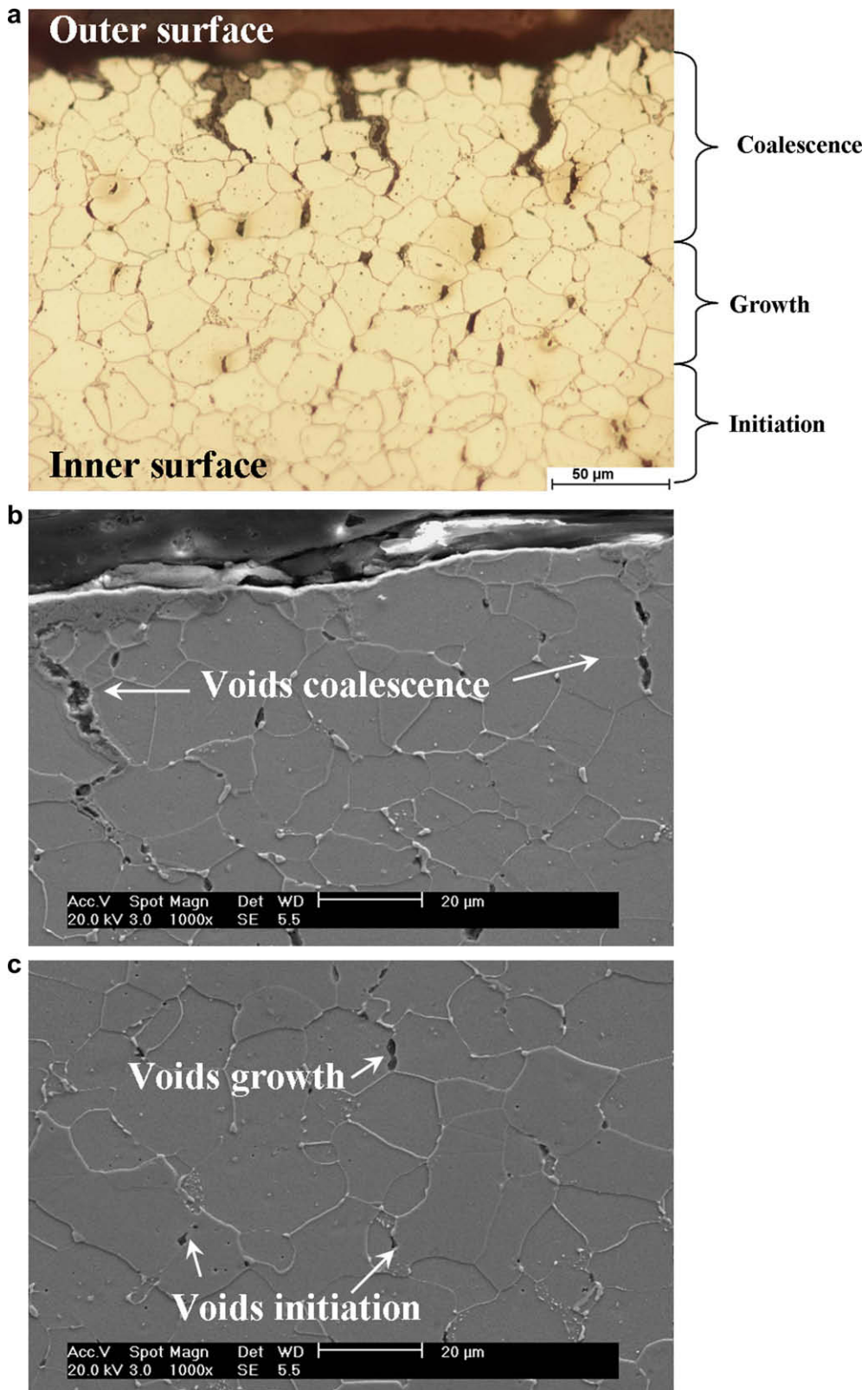


**Fig. 3.** Cross-sections along the line BB' of Fig. 1b: (a) optical micrograph of the failed-tube wall; (b) SEM image of outer surface of the failed-tube wall and (c) SEM image of inner surface of the failed-tube wall.

### 3.1. Failure at the curved areas of the pipeline

The failed parts retrieved from curved pipeline areas exhibit the typical “fish-mouth” thin-lip rupture (Fig. 1a), commonly observed in cases of creep-induced failure of superheater and reformer tubes [3,4].

In the particular case, rupture occurred always at the inner wall of the curved tube. The wall thickness at the tip of the “fish-mouth” was diminished from its original value of 6 mm down to about 1 mm, whilst the typical metal plastic flow striations could also be clearly observed along the tube axis (Fig. 1b). At a distance of about 30 mm from the rupture tip, a bump on

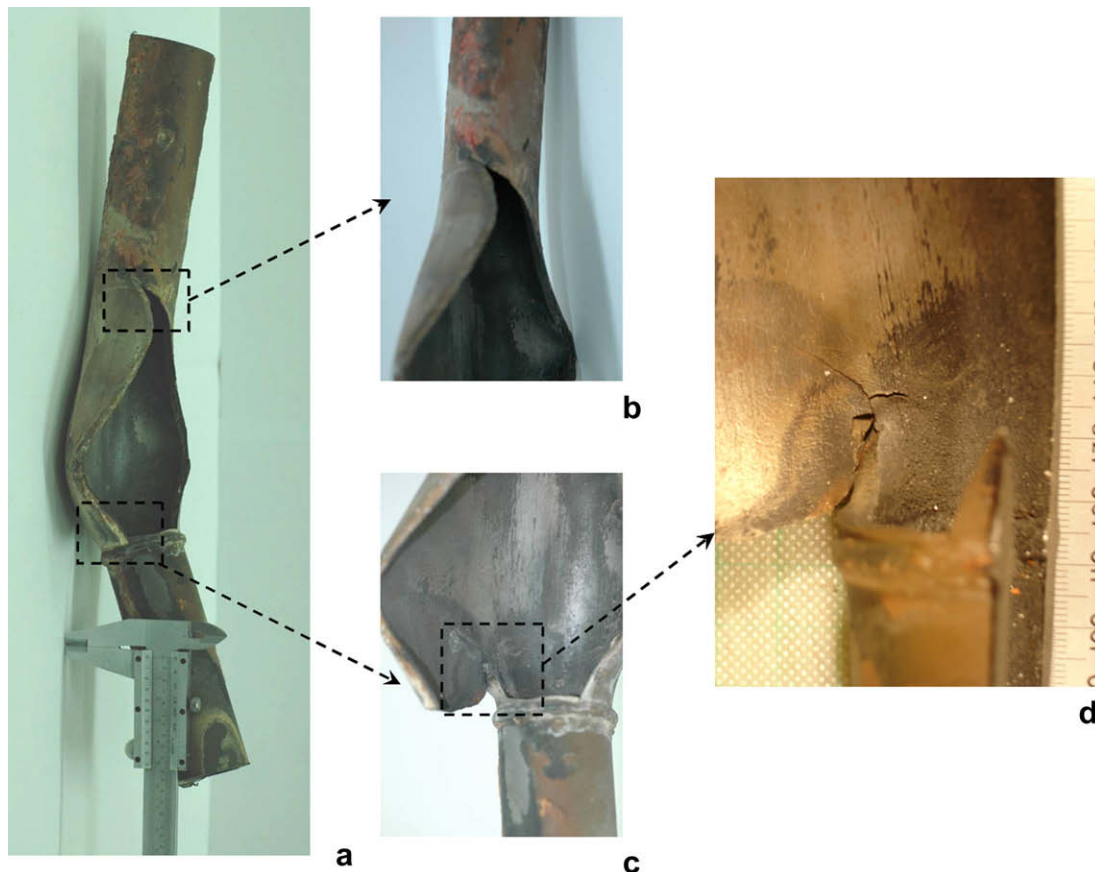


**Fig. 4.** Macrographs of the failed-tube retrieved from area of the pipeline with circumferential weldment: (a) total view of the retrieved part, exhibiting a “cobra” appearance and (b-d) zooming of characteristic areas, indicated in (a).

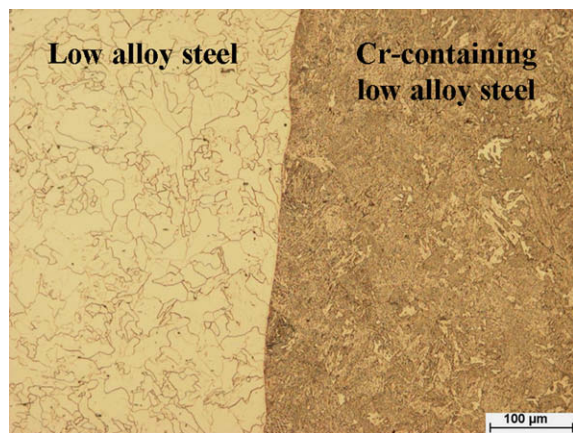


**Fig. 5.** Optical micrograph of a cross-section perpendicular to the circumferential weldment, revealing solid-state welding of dissimilar steel grades.

the inner wall had occurred, partially covered by a characteristic oxide layer (Fig. 1c, brown areas) exhibiting an “orange-peel” effect. On the oxide layer, yawning of intermittent secondary rupture cracks in the direction of the tube axis can be recognised. The secondary rupture cracks can be also observed as slight openings (Fig. 1c), at areas where the base metal is revealed due to

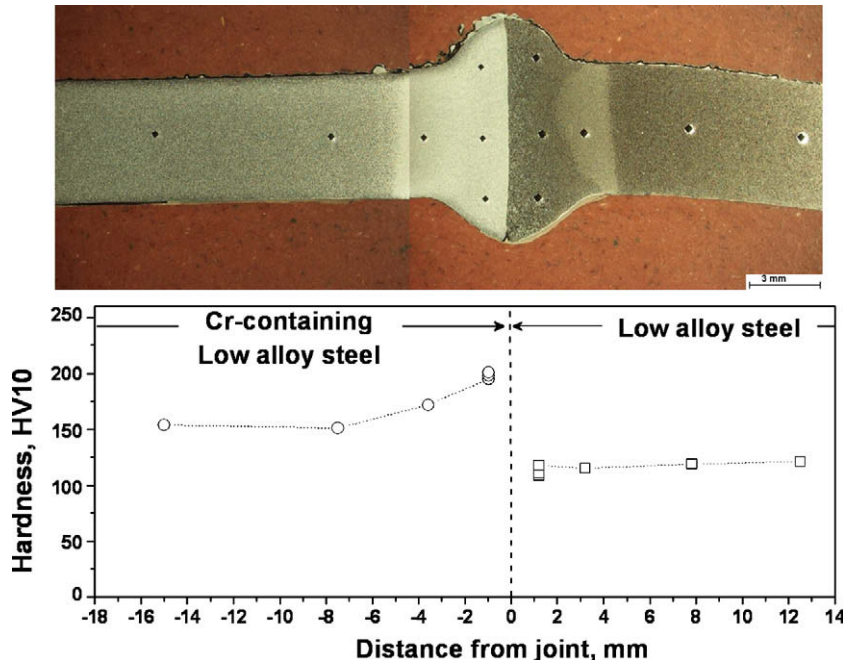


**Fig. 6.** Stereo-graph of a cross-section perpendicular to the circumferential weldment, areas and values of the Vickers hardness measurements performed.

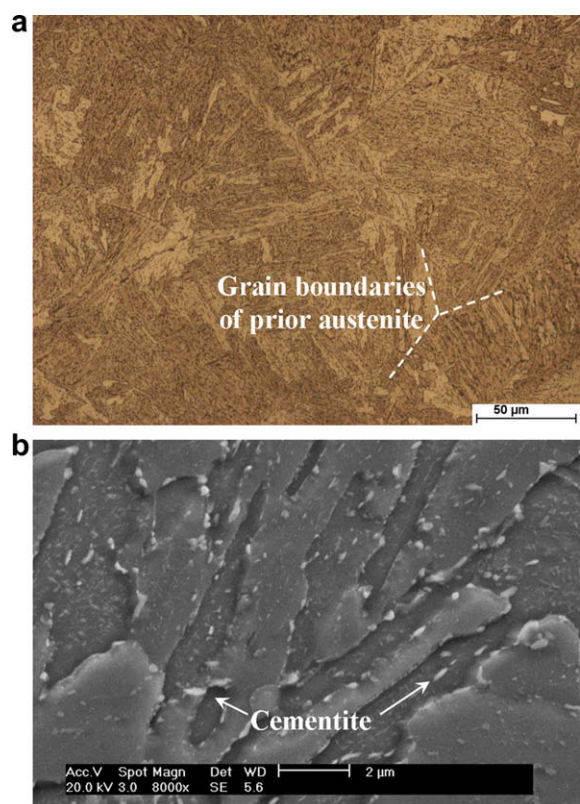


**Fig. 7.** Optical (a) and SEM (b) images of the Cr-containing steel grade, from cross-sections in the neighbourhood of the joint boundary.

detachment of the cracked oxide layer, most likely caused during the maintenance works. Similar features have been observed in the case of creep failure of turbine blades [5]. Such oxide layers were also present on the diametrically opposite area of the outer wall of the curved tube; however they were much thinner, free of cracks and well adhered to the parent metal. Wall thinning extending to a distance of about 120 mm from the rupture tip was observed; at this location the thickness of the inner wall was measured at 4 mm, corresponding to a 33% reduction of its original dimension (Fig. 1d).

Stereo- and SEM-photographs of the rupture-lips' (Fig. 1b, marked area) are shown in Fig. 2. On the dimpled fracture surface (Fig. 2b), two co-existing features can be clearly distinguished:

- Large equiaxial voids arising from the coalescence of creep voids of smaller dimensions (Fig. 2c).
- Elongated dimples corresponding to the initial orientation of the material's grains due to the unidirectional tube forming process (Fig. 2d).

The creep void evolution across the tube wall is presented in Fig. 3a. At the outer surface of the tube, void coalescence (Fig. 3b) resulted in intergranular surface cracks of a mean length of 50 µm, filled with oxidation products. Consequently, a second zone of creep void growth can be observed, extending from a depth of about 70 µm to about 130 µm (Fig. 3c); whilst toward the inner surface of the wall, initiation of individual voids appeared along the grain boundaries (Fig. 3c) [6,7]. The co-existence on the same tube cross-section of the three stages in creep void evolution: initiation/growth/coalescence is indicative of a temperature gradient across the wall through which heat exchange is taking place between the hot lignite combustion gases in contact with the outer surface of the tube and the high-pressure steam flow in contact with the inner surface of the tube.

The tube material identification was obtained by applying both metallographic observation and EDAX microanalysis; which showed that it was a low-alloy ferritic steel, probably corresponding to the 15Mo3 grade proposed by the designers of the pipeline. Precipitates observed at the grain boundaries (Fig. 3b and c) indicated cementite spheroidisation, due to the prolonged heating of the material during operation, at a temperature close to  $A_{C1}$ .

### 3.2. Failure in the neighbourhood of welding seams

The failed parts of the pipeline retrieved from areas near circumferential weldments (Fig. 4) exhibit a "cobra" appearance [3], with fracture cracks initiating near the seam (Fig. 4c) and propagating within one of the joined tubes, in a direction almost parallel to its axis (Fig. 4d).

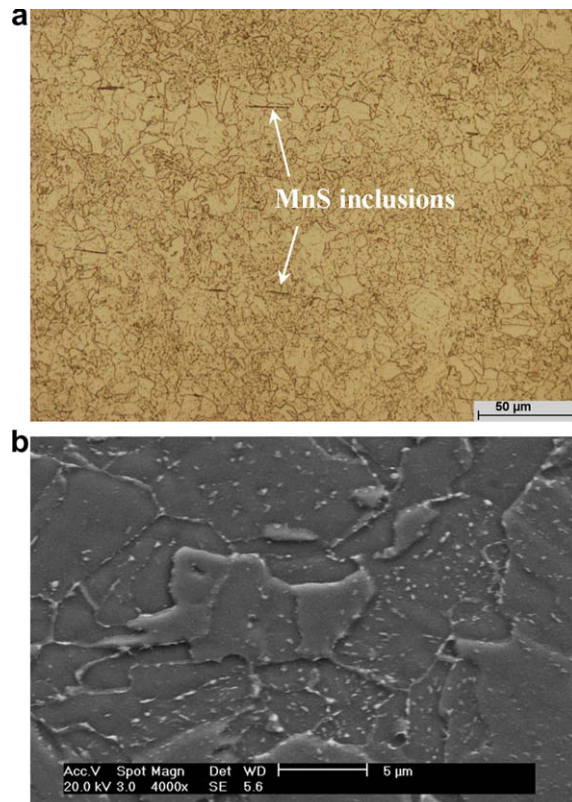


**Fig. 8.** Optical (a) and SEM (b) images of the Cr-containing steel grade, from cross-sections at an area of intermediate hardness.

Metallographic observations of the weldment's cross-section (Fig. 5) revealed both the materials' dissimilarity of the joined tubes, as well as the absence of fusion zone or filler material, which indicate that a high-temperature solid-state welding technique was applied. EDAX microanalysis indicated that one of the tubes was a Cr-containing steel, probably corresponding to the 13CrMo44 or 10CrMo910 grades also proposed by the designers, whilst the other one, within which fracture cracks had propagated, was a low-alloy ferritic steel, as in the previous case. Although there is a clear boundary between the two welded parts and there is no apparent metallurgical bonding between the two joined surfaces, the seam nevertheless can be characterised as one of excellent quality, since failure initiation was clearly located outside of it.

Vickers hardness measurements performed along the direction of the tube's axis (perpendicular to the seam, Fig. 6) revealed a substantial drop in hardness values between the two sides adjacent to the seam:

- In the case of Cr-containing steel grade, the area near the seam exhibited a mean hardness of 200 HV10; at a distance of 3.5 mm from it the value dropped to 170 HV10 and further away, to that of the parent material ( $\sim$ 150 HV10).
- In the case of ferritic steel, hardness exhibited a slight increase from 110 HV10 near the seam to 120 HV10 at the parent material.

The solid-state metallurgical transformations, attributed to both the welding process as well as to the high-temperature service conditions, that led to the above hardness distribution were extensively studied by metallography and SEM observations.

In the case of Cr-containing steel grade, the area close to the joint boundary, of 2 mm width, exhibited no re-solidification features, but had the characteristic upper-bainite structure (Fig. 7), with the grain boundaries of prior austenite clearly distinguished. The adjacent area of intermediate hardness of 2.5 mm width, consisted of tempered ferrite with a fine distribution of spheroidised cementite (Fig. 8). Finally, the parent material had a microstructure of ferrite with partially spheroidised pearlite (Fig. 9). Oblong dark features within the base structure correspond to MnS inclusions, entrapped during the material production and shaped during the tube forming process.

In the case of ferritic steel, the area close to the joint boundary, of 2 mm width, presented irregular ferrite grains (Fig. 10), while dark precipitations distributed within the base microstructure corresponded to residual fluxes ( $\text{Al}_2\text{O}_3$  and/or  $\text{CaO}$ ) that were entrapped during solidification of the raw material and spheroidised due to their high surface tension. The adjacent

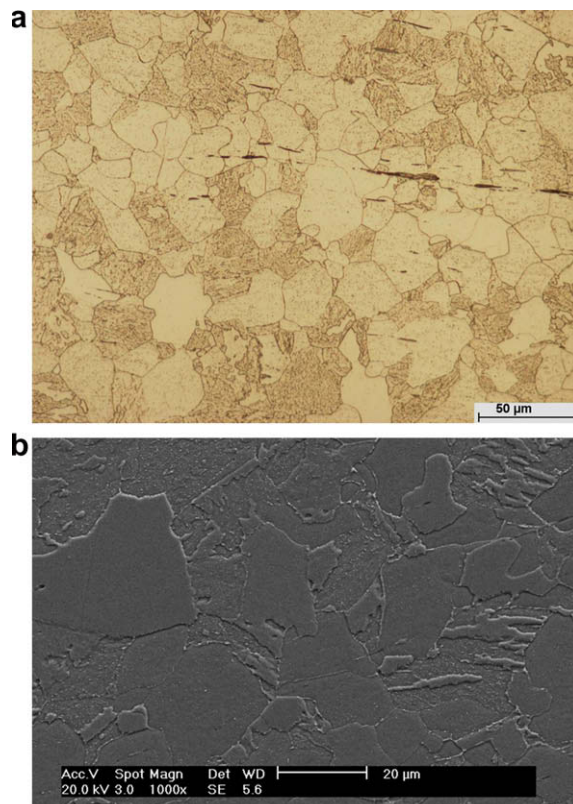


**Fig. 9.** Optical (a) and SEM (b) images of the Cr-containing steel grade initial structure.

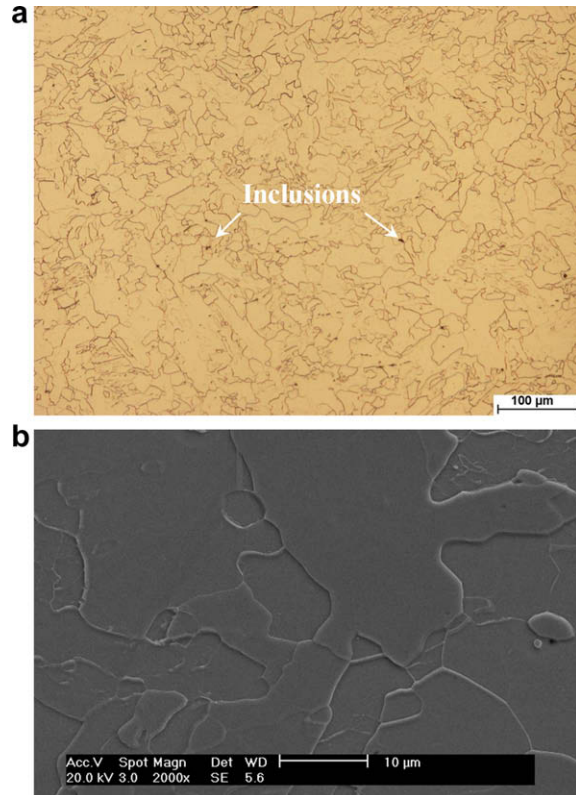


**Fig. 10.** Optical (a) and SEM (b) images of the ferritic steel, from cross-sections in the neighbourhood of the joint boundary.

area of 2.5 mm width also consisted of equiaxial ferrite grains, of uniform distribution, which indicates that the material was re-crystallised (Fig. 11). The carbide precipitates found at the grain boundaries probably correspond to spheroidised cementite. In the same area, individual creep voids of small size were scarcely observed. The parent structure was characterised by ferrite grains (normalised ferrite) and a high distribution of creep voids (Fig. 12).

Compared to the area of re-crystallised ferrite, the parent material exhibited large ferrite grains, of almost double the size; and round, trans-granular creep voids with an average diameter of 0.05 mm (Fig. 13a). A close view on this area revealed that the growth and coalescence of creep voids was taking place through micro-necking between two adjacent voids of crucial size (Fig. 13b). Around the voids at this area, a circular zone can be observed with clear evidence of the material dynamic re-crystallisation (Fig. 13a and b), which is attributed to ferrite straining caused during void growth.

#### 4. Discussion and conclusions

In the present study, the metallurgical modifications taking place during high-temperature exposure of a steel pipeline that led to local material's failure were investigated. Failure was localised either at curved areas of the tubes, or in the neighbourhood of circumferential weldments and the failed parts exhibited a "fish-mouth" or a "cobra" appearance respectively, morphologies characteristic of creep rupture. The short-time service-life (~15 days of continuous operation) indicated the absence of a primary creep stage, commonly appearing in cases of operation under conditions of a high-temperature and/or high stress regime.

- Since no data on the actual steam pressure were available and considering that there was no deviation from the design, the hoop stress was estimated at 50.5–51.5 MPa, via the Lamé equation valid for thick-wall tubes.
- The initial design of the pipeline has taken into account that steam inlet and outlet temperature were respectively 35.5% and 39.6% of the material's melting point; whilst during service these parameters were higher: 39.9% and 43.0%.
- In both failure cases presented above, rupture always took place within low-alloy ferritic steel, probably corresponding to 13Mo3 grade; whilst the presence of impurities like oblong MnS and round Al<sub>2</sub>O<sub>3</sub>, CaO did not seem to affect the creep behaviour of the material.

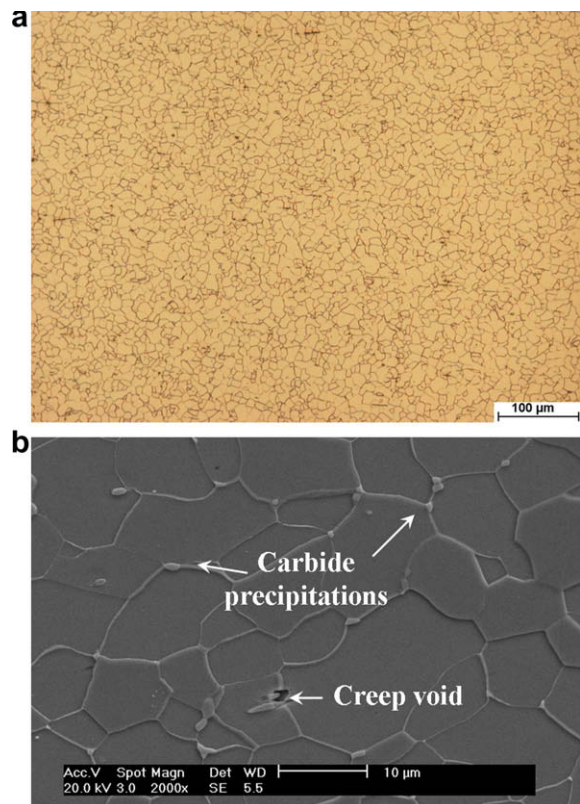


**Fig. 11.** Optical (a) and SEM (b) images of the ferritic steel, revealing material's re-crystallisation.

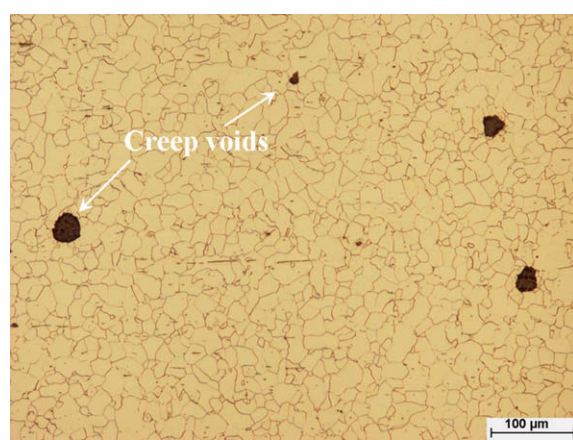


**Fig. 12.** Optical micrograph of initial structure of the ferritic steel.

Based on these points, the continuous pipeline review and re-design is suggested taking into account each time the calorific value of lignite that is fed to the combustion chamber of the unit. As this seems to be higher with increasing exploitation depth, the 13Mo3 grade should be rejected and more heat-resistant steel grades should be considered as materials of choice.

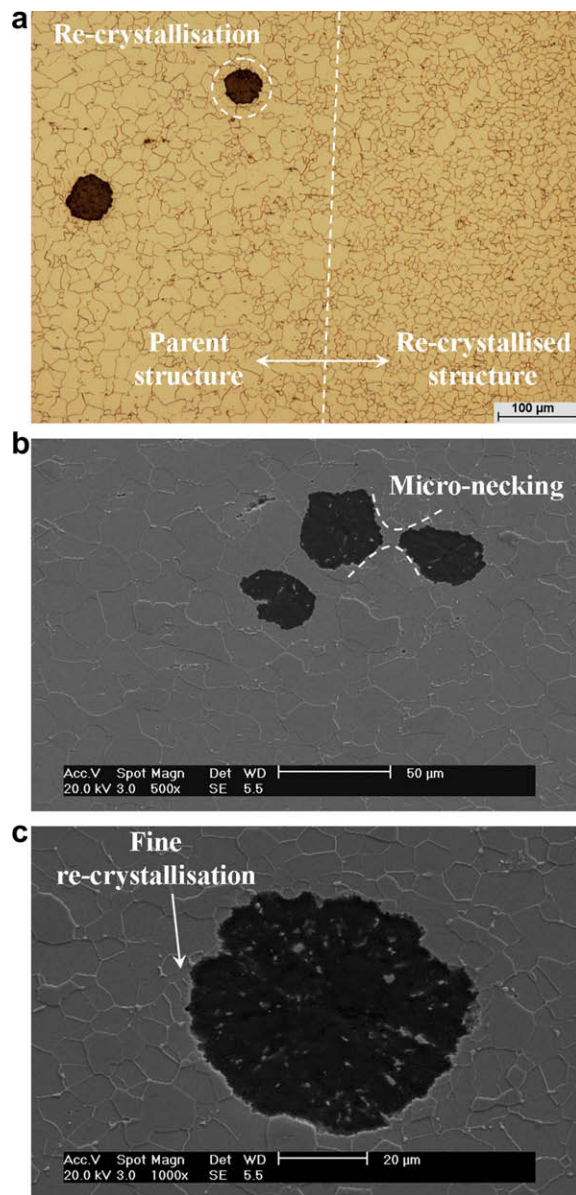


**Fig. 13.** (a) Optical micrograph of the boundary of the re-crystallised/initial structure of the low-alloy steel grade; (b) SEM micrograph of the parent material, indicating micro-necking between adjacent creep void and (c) SEM micrograph of the parent material, indicating fine dynamic re-crystallisation around a creep void.

887799

# Materials safety: article exercise

You are working as a materials expert in your organization and your responsibility is to guarantee safe and efficient use of materials in your facility. One day, a failure in similar facility is brought to your attention, and you need to investigate the possible implications this failure has for your facility. Your job is to interpret and analyze the given failure report and to write a report, which will allow others in your organization to understand the key developments and causes leading to the failure and the necessary actions for prevention of such failures.

Read the given article and analyze the failure. Describe, how the deformation and failure mechanisms presented during the course are reflected in the case and establish the chain of actions leading to the failure. The report should work as an introductory material to your team; it should not be very long but it should enable other team members to understand the key features of the failure without reading the failure report itself.

In addition to establishing the primary cause of the failure, show why alternate failure mechanisms can be ruled out. Some failure mechanisms have not been discussed in the course yet. Conduct the analysis using your present knowledge on the subject.

If the author of the failure analysis has, in your view, neglected to address some aspects of the failure, you may indicate this in your report and suggest tests or actions that should have been done to clarify the issue.

Prepare your response by editing this word document and export it as PDF. The file name identifies you and the article. Do not change the file name (other than the extension to pdf). E-mail the pdf to "materials.safety@iikka.fi".

You may use the question list below to guide you in your analysis:

**A. Description of investigation methods applied**

- What means of investigation were used in the failure analysis?
- What computational methods were used?
- What material or results were obtained?

**B. The primary cause of the failure and description of the failure mechanism**

- What is the primary cause of the failure (also provide reasoning)?
- What's the chain of action that led to the failure?

**C. Ruling out alternate failure mechanisms**

- Can plastic deformation be ruled out? If yes, explain how.
- Can creep be ruled out? If yes, explain how.
- Can brittle fracture be ruled out? If yes, explain how.
- Can fatigue be ruled out? If yes, explain how.
- Can environmentally assisted failure be ruled out? If yes, explain how.

**D. Recommendations to prevent similar failures in the future**

- How should the design, material, use, etc. be developed to avoid similar failures in the future? Provide several alternatives and indicate most promising.

Name: Nguyen Xuan Binh  
Student ID: 887799

## Materials Safety analysis report on creep failure of superheater tubes

### Problem Overview:

The report investigated the reasons why certain superheater tubes kept failing over time. They observed a recurring "fish-mouth" type of rupture in these tubes, especially in the curved areas. By examining the tubes' structure and materials, they aimed to uncover the causes of these failures. Their insights offer guidance for future design improvements to ensure safer and more efficient heating systems and to reduce maintenance time interval and costs.

### A. Description of investigation methods applied

- **What means of investigation were used in the failure analysis?**

The author tries to determine whether creep and environmentally induced factors are associated with the fish-mouth shaped failures observed in superheater tubes. From the report, the means of investigation for the failure analysis included:

1. **Macroscopic observations:** The author used a Leica MS 5 and a Nikon SMZ 1500 stereomicroscope to perform macroscopic observations of the failed tubes.
2. **Microscopic observations:** An FEI XL40 SFESEM scanning electron microscope (SEM) equipped with an electron dispersive spectrometry X-ray microanalysis system (EDAX) was utilized for microscopic observations.
3. **Metallographic examination:** A Nikon Epiphot 300 inverted metallurgical microscope was used for metallographic examination. Before this examination, cross-sections of the failed tubes were prepared using hot-mounting, wet grinding up to 1200 grit SiC paper, and polishing with diamond and silica suspensions.
4. **Chemical etching:** The specimens were chemically etched by immersion in a Nital reagent (2% HNO<sub>3</sub> ethanol solution) for 10 seconds. This was followed by cleaning with ethanol and drying with a hot-air streams

- **What computational methods were used?**

The author lists a couple of computation methods as follows:

1. **Optical Micrographs:** These provide detailed images of the material's structure, allowing for a closer look at the grain boundaries, voids, and other microstructural features. For instance, the paper shows optical micrographs of the failed-tube wall
2. **SEM (Scanning Electron Microscopy) Images:** SEM records high-resolution images of the material's surface. The report contains several SEM images, such as those revealing the material's recrystallization and the initial structure of the Cr-containing steel grade
3. **Stereographs:** These are used to provide a three-dimensional view of the material's structure. The paper references a stereograph of a cross-section perpendicular to the circumferential weldment, showing values of the Vickers hardness measurements.
4. **Vickers hardness measurements:** The paper mentions the use of Vickers hardness measurements to determine the material's hardness at specific areas, especially in the vicinity of weldments.

- **What material or results were obtained?**

**Main result:** Failure is identified at the curved areas of the pipeline

The failed parts exhibited a "fish-mouth" thin-lip rupture, commonly observed in creep-induced failures of superheater and reformer tubes. Rupture always occurred at the inner wall of the tube, with the wall thickness at the tip diminishing from the original 6 mm to about 1 mm. Failed parts from areas near circumferential weldments exhibited a "cobra" appearance.

**Material Identification:** The tube material was identified as a low-alloy ferritic steel, likely corresponding to the 15Mo3 grade. This identification was based on metallographic observation and EDAX microanalysis.

## B. The primary cause of the failure and description of the failure mechanism

- **What is the primary cause of the failure (also provide reasoning)?**

The primary cause of the failure is likely to be creep-induced failure. There are four main reasons for this type of failure:

- The failed parts displayed a "fish-mouth" thin-lip rupture, which is commonly observed in cases of creep-induced failure of superheater and reformer tubes.
- Precipitates at the grain boundaries indicated cementite spheroidization, resulting from the prolonged heating during operation. This can accelerate creep behavior.
- Different stages of creep void evolution on the same tube cross-section (initiation, growth, and coalescence) suggest a temperature gradient across the tube wall, which can enhance creep deformation and eventual failure.
- Failed parts near circumferential weldments displayed a "cobra" appearance. Welded areas are susceptible to creep-induced failure due to residual stresses and microstructural changes between the two alloys from the welding process.

- **What's the chain of action that led to the failure?**

The chronological order of the superheater tubes' failure is as follows:

1. Prolonged heating and material transformation: The tube underwent prolonged heating during operation. This led to cementite spheroidization, a material transformation observed at the grain boundaries.
2. Temperature gradient across the tube wall: This gradient led to the co-existence of different stages of creep void evolution on the same tube cross-section, including initiation, growth, and coalescence of voids.
3. Failure near welding seams: fracture cracks initiating near the seam and propagating within one of the joined tubes, almost parallel to the main axis.
4. Systematic Recording of Failures: data recorded over one year of the pipeline's service showed that material failures occurred on average every 15 days. These failures were localized either at curved areas of the tubes or near circumferential weldments.

## C. Ruling out alternate failure mechanisms

- Can plastic deformation be ruled out? If yes, explain how.

The paper mentions the observation of "metal plastic flow striations" along the tube axis, especially in the curved areas of the pipeline. This suggests that there was some form of plastic deformation prior to failure. However, this plastic flow is probably a result from the creep mechanism rather than conventional plastic deformation. So plastic deformation as the main failure mechanisms can be ruled out.

- Can creep be ruled out? If yes, explain how.

Creep cannot be ruled out since this is one of the main failure reasons stated in the paper

- Can brittle fracture be ruled out? If yes, explain how.

Brittle fracture can be ruled out since the material deformation is observed to be quite ductile (void nucleation, growth, and coalescence).

- Can fatigue be ruled out? If yes, explain how.

Fatigue cannot be ruled out. The superheater tubes operate under high temperatures and pressures, conditions that are conducive to creep. However, the frequent interruptions for maintenance and potential alternations in steam pressure could introduce cyclic thermal stresses, which are a sign of fatigue. Therefore, fatigue should be considered in this report as well.

- Can environmentally assisted failure be ruled out? If yes, explain how.

Environmentally assisted failure cannot be ruled out since this is one of the main failure reasons stated in the paper, such as temperature gradient and material phase transformation.

#### D. Recommendations to prevent similar failures in the future

- How should the design, material, use, etc. be developed to avoid similar failures in the future? Provide several alternatives and indicate the most promising.

To avoid similar failures in the future, several design, material, and usage recommendations can be inferred from the paper:

1. Material selection: As the calorific value of lignite seems to increase with exploitation depth, the 13Mo3 steel grade should be rejected. Instead, more heat-resistant steel grades should be considered as materials of choice to withstand the high temperatures and stresses experienced in such environments.
2. Improved welding techniques: given that some failures were observed near welding seams, it might be beneficial to explore improved welding techniques or materials that can better withstand the operating conditions of superheater tubes.
3. Monitoring and maintenance: regular monitoring of the pipeline's condition and performance can help detect early signs of potential failures. This includes checking for signs of creep, material transformation, and other microstructure anomalies.

101843742

# Materials safety: article exercise

You are working as a materials expert in your organization and your responsibility is to guarantee safe and efficient use of materials in your facility. One day, a failure in similar facility is brought to your attention, and you need to investigate the possible implications this failure has for your facility. Your job is to interpret and analyze the given failure report and to write a report, which will allow others in your organization to understand the key developments and causes leading to the failure and the necessary actions for prevention of such failures.

Read the given article and analyze the failure. Describe, how the deformation and failure mechanisms presented during the course are reflected in the case and establish the chain of actions leading to the failure. The report should work as an introductory material to your team; it should not be very long but it should enable other team members to understand the key features of the failure without reading the failure report itself.

In addition to establishing the primary cause of the failure, show why alternate failure mechanisms can be ruled out. Some failure mechanisms have not been discussed in the course yet. Conduct the analysis using your present knowledge on the subject.

If the author of the failure analysis has, in your view, neglected to address some aspects of the failure, you may indicate this in your report and suggest tests or actions that should have been done to clarify the issue.

Prepare your response by editing this word document and export it as PDF. The file name identifies you and the article. Do not change the file name (other than the extension to pdf). E-mail the pdf to "materials.safety@iikka.fi".

You may use the question list below to guide you in your analysis:

**A. Description of investigation methods applied**

- **What means of investigation were used in the failure analysis?**
  - Macroscopic Observations: Stereomicroscope (Leica MS 5) and Nikon SMZ 1500 stereomicroscope were used for macroscopic observations of the failed tubes.
  - Microscopic Observations: Microscopic observations were carried out using an FEI XL40 SFESEM scanning electron microscope (SEM) equipped with an electron dispersive spectrometry X-ray microanalysis system (EDAX) for elemental analysis of selected areas.
  - Metallographic Examination: A Nikon Epiphot 300 inverted metallurgical microscope was used for metallographic examination. Cross-sections of the failed tubes were prepared using hot-mounting, wet grinding up to 1200 grit SiC paper, and polishing with diamond and silica suspensions.
  - Hardness Measurements: Vickers hardness measurements on characteristic areas of the welded specimens were carried out using an Instron-Wolpert tester, applying a load of 10 kg.
- **What computational methods were used?**

The computational methods used in the analysis were not explicitly mentioned in the text.

• **What material or results were obtained?**

The materials identified in the investigation included low-alloy ferritic steel, possibly corresponding to the 15Mo3 grade, and Cr-containing steel, probably corresponding to the 13CrMo44 or 10CrMo910 grades. The results of the investigation revealed microstructural changes, creep void evolution, and material transformations associated with high-temperature exposure, providing insights into the failure mechanisms.

**B. The primary cause of the failure and description of the failure mechanism**

- **What is the primary cause of the failure (also provide reasoning)?**

Creep rupture due to elevated temperatures and abnormal operating conditions. The material wasn't suitable for high temperatures.
- **What's the chain of action that led to the failure?**

Elevated temperatures, continuous operation, inappropriate material, and creep rupture.

**C. Ruling out alternate failure mechanisms**

- **Can plastic deformation be ruled out? If yes, explain how.**

The failure exhibited characteristics of ductile creep rupture, such as necking and void formation, inconsistent with plastic deformation.
- **Can creep be ruled out? If yes, explain how.**

Creep was identified as the primary failure mechanism due to material behavior under elevated temperatures, supported by microscopic evidence.
- **Can brittle fracture be ruled out? If yes, explain how.**

The failure displayed characteristics of ductile creep rupture, including necking and void formation, incompatible with brittle fracture.

- **Can fatigue be ruled out? If yes, explain how.**

Fatigue was not a contributing factor; failure resulted from continuous operation under high temperatures and showed no fatigue-related features.

- **Can environmentally assisted failure be ruled out? If yes, explain how.**

Creep failure was directly influenced by environmental conditions such as high temperature. Therefore, it is a reason for its failure.

**D. Recommendations to prevent similar failures in the future**

- **How should the design, material, use, etc. be develop to avoid similar failures in the future? Provide several alternatives and indicate most promising.**

Some ideas to prevent similar failures are select heat-resistant materials, conduct regular inspections, maintain optimal temperatures, explore high-alloy steels, and implement efficient maintenance strategies to prevent future failures.

712712

# Materials safety: article exercise

You are working as a materials expert in your organization and your responsibility is to guarantee safe and efficient use of materials in your facility. One day, a failure in similar facility is brought to your attention, and you need to investigate the possible implications this failure has for your facility. Your job is to interpret and analyze the given failure report and to write a report, which will allow others in your organization to understand the key developments and causes leading to the failure and the necessary actions for prevention of such failures.

Read the given article and analyze the failure. Describe, how the deformation and failure mechanisms presented during the course are reflected in the case and establish the chain of actions leading to the failure. The report should work as an introductory material to your team; it should not be very long but it should enable other team members to understand the key features of the failure without reading the failure report itself.

In addition to establishing the primary cause of the failure, show why alternate failure mechanisms can be ruled out. Some failure mechanisms have not been discussed in the course yet. Conduct the analysis using your present knowledge on the subject.

If the author of the failure analysis has, in your view, neglected to address some aspects of the failure, you may indicate this in your report and suggest tests or actions that should have been done to clarify the issue.

Prepare your response by editing this word document and export it as PDF. The file name identifies you and the article. Do not change the file name (other than the extension to pdf). E-mail the pdf to "materials.safety@iikka.fi".

You may use the question list below to guide you in your analysis:

**A. Description of investigation methods applied**

- What means of investigation were used in the failure analysis?
  - Macroscopic and microscopic observations of the failed specimen
  - Hardness testing
  - Thickness and other dimensional measurements
  - Information on failure frequency of the part
  - Measurements of operating conditions like pressure and temperature
- What computational methods were used?
  - 1. Stereomicroscopy for macroscopic observation
  - 2. SEM for microscopic structure analysis
  - 3. EDAX for elemental analysis
- What material or results were obtained?
  -

**B. The primary cause of the failure and description of the failure mechanism**

- What is the primary cause of the failure (also provide reasoning)?
  - Creep rupture caused by high temperature and pressure operating environment.
- What's the chain of action that led to the failure?
  - 30 years of service in high temperature and pressure -> creep void formation -> micro-necking between voids -> coalescence of voids into larger voids -> increased stress resulting in rupture failure.

**C. Ruling out alternate failure mechanisms**

- Can plastic deformation be ruled out? If yes, explain how.
  - Most likely. The material has operated for 30 years with no significant changes to stresses affecting it. The materials are stressed well below their yield points.
- Can creep be ruled out? If yes, explain how.
  - Creep is the method of failure.
- Can brittle fracture be ruled out? If yes, explain how.
  - Yes. The swelling of the tube indicates ductile not brittle behavior of the material. Hardness tests support this notion.
- Can fatigue be ruled out? If yes, explain how.
  - Most likely. The operating conditions are fairly stable in a powerplant and as a result any cyclical pressure or temperature loads should not cause a great enough number of fatigue cycles. There are also no tell-tale beach marks.
- Can environmentally assisted failure be ruled out? If yes, explain how.

- The failures occur consistently in the same parts of the super heater pipes. If environmentally assisted failure played a major role, material issues would likely show up in other parts as well.

D. Recommendations to prevent similar failures in the future

- How should the design, material, use, etc. be developed to avoid similar failures in the future? Provide several alternatives and indicate most promising.
  - The current superheater piping is clearly at the end of its lifespan. Therefore, full replacement is the only sensible option. Higher heat resistance steel should be considered for the replacement if economical. Otherwise replacing the superheater with a new one made of the same materials may be reasonable considering the 30-year service life the previous one achieved. An even lower grade material might be possible if the plant has a limited lifetime ahead of it.

100603611

# Materials safety: article exercise

You are working as a materials expert in your organization and your responsibility is to guarantee safe and efficient use of materials in your facility. One day, a failure in similar facility is brought to your attention, and you need to investigate the possible implications this failure has for your facility. Your job is to interpret and analyze the given failure report and to write a report, which will allow others in your organization to understand the key developments and causes leading to the failure and the necessary actions for prevention of such failures.

Read the given article and analyze the failure. Describe, how the deformation and failure mechanisms presented during the course are reflected in the case and establish the chain of actions leading to the failure. The report should work as an introductory material to your team; it should not be very long but it should enable other team members to understand the key features of the failure without reading the failure report itself.

In addition to establishing the primary cause of the failure, show why alternate failure mechanisms can be ruled out. Some failure mechanisms have not been discussed in the course yet. Conduct the analysis using your present knowledge on the subject.

If the author of the failure analysis has, in your view, neglected to address some aspects of the failure, you may indicate this in your report and suggest tests or actions that should have been done to clarify the issue.

Prepare your response by editing this word document and export it as PDF. The file name identifies you and the article. Do not change the file name (other than the extension to pdf). E-mail the pdf to "materials.safety@iikka.fi".

You may use the question list below to guide you in your analysis:

A. Description of investigation methods applied

- What means of investigation were used in the failure analysis?
  - To analyze the failed material, macroscopic observation was done using Leica MS 5 and Nikon SMZ 1500 stereomicroscopes.
  - FEI XL40 SFEG SEM microscope with EDAX was used to reveal the failure mechanisms in elementary areas.
  - For metallographic examination, Nikon Epiphot 300 inverted metallurgical microscope was used.
  - To investigate the cross sections of the failed tube, hot mounting was used, and the cross sections were polished.
  - Etching of the pieces were done by submerging them in 2% HNO<sub>3</sub> for 10 seconds, then cleaning with ethanol and drying with hot air.
  - Hardness testing were done by using Vickers hardness test on characteristic areas of welded specimens, by Instron-Wolpert tester.

B. The primary cause of the failure and description of the failure mechanism

- What is the primary cause of the failure (also provide reasoning)?
- The failure occurred mostly because of the high temperatures, to which the materials of the tubes were exposed. Also, the high stress areas were prone to failure.
- The growth of the voids towards the outer surface of the tube wall were indicating temperature gradient through the wall of the tube, where hot ignition gases are present in the outer surface and the high pressure steam flow inside the tube.
- The material selection also seems to have affected to the crack propagation. The material of the tube wall, where the void evolution was observed, had been low-alloy ferritic steel (probably 15Mo3).

- The cracks in the tubes were retrieving from the circumferential weldments and it was found that the material of the joined tubes weren't the same. The other of the materials, in which the cracks had propagated, was low-alloy ferritic steel, similarly than in the tube wall in which the void growth had occurred.

**C. Ruling out alternate failure mechanisms**

- Can plastic deformation be ruled out? If yes, explain how.
- Can creep be ruled out? If yes, explain how.
- Can brittle fracture be ruled out? If yes, explain how.
- Can fatigue be ruled out? If yes, explain how.
- Can environmentally assisted failure be ruled out? If yes, explain how.

**D. Recommendations to prevent similar failures in the future**

- How should the design, material, use, etc. be develop to avoid similar failures in the future? Provide several alternatives and indicate most promising.
- To prevent similar failures from happening in the future, the low-alloy ferritic steel structures shall be changed to alloy, in which the voids wouldn't grow because of the temperature gradient across the tube wall. Materials in high stress areas and materials near the welded seams shall be chosen to be more temperature resistant. These would be the most important.
- The steam temperature shall be adjusted to fit the designed temperatures, since they were significantly higher than designed values.
- The chemical composition of the gas could be stabilized if possible.



100488467

# Materials safety: article exercise

## Background

The study investigates systematic short-time failure of a superheater pipeline, which were part of the steam operating main heat exchanger assembly of a powerplant located in Northern Greece. The pipeline was constructed over a lignite combustor 30 years ago. The original design of the multi-curved pipeline was built up by an array of individual tubes with outer diameter 38mm, wall thickness 6mm, and length 4m. The tubes were welded together to form the pipeline of a heat exchange area of 5200 mm<sup>2</sup>. Construction materials were the following steel grades: 15Mo3, 13MoCr44, and 10CrMo910, which all are typical material choices for pressure vessels. A high frequency of costly maintenance, reparation, and replacement of failed pipeline parts was observed during several years, resulting in limiting operations and costly downtime of plant. An average of 15 days of continuous operation were eventually reached due to the continuous failures.

## Investigation methods

To identify failure mechanism of the pipeline, metallurgical investigations were conducted of failed parts. Systematic data recording of failures was carried out during a period of over one year. The experimental techniques included the following:

- Macroscopic observation of failed tubes using a stereomicroscope
- Microscopic observation using scanning electron microscope (SEM) equipped with electron dispersive spectrometry X-ray microanalysis system (EDAX) for elemental analysis
- Metallographic examination using inverted metallurgic microscope
- Chemical etching
- Vickers hardness measurements on welded specimens

Results from the failure analysis showed that local material failure occurred with an average of 15 days. Failures were located either at curved areas of the tubes or close to circumferential weldments.

## Primary cause of failure

The metallurgical changes occurring during the high-temperature exposure of this steel pipeline resulted in material failures. The failures were located at curved areas and close to circumferential weldments, and the morphological characteristics of these failures indicated characteristics of creep rupture. Since there was a short service life, it was indicated an absence of primary creep stage. The article argues that this is commonly seen in cases of operation conditions of high-temperature and/or high stress regime.

## Alternate failure mechanisms

Plastic deformation can be ruled out since the article mentions no indications of plastic deformation found from investigations.

Brittle fracture can be ruled out since that is characterized by sudden failure without significant deformation. The failure analysis in this case showed several deformations related to the failures.

Several crack propagations were found during the study, so fatigue could be an alternate failure mechanism. The pipelines were subjected to operating conditions (temperature and possibly pressure) not conforming to the design guidelines.

Environmentally assisted failure can be ruled out since the article did not mention any signs of environmental impact on the pipeline.

## Prevention of similar failures

Pipeline review and re-design was recommended by the article, as well as selecting more heat-resistant steel grades for material choice. Operating pressure was missing from the investigation. This would be beneficial to determine, to further examine whether sufficient design pressure was considered during development of the pipeline. Service temperatures of steam inlet and outlet were also higher than initial design guidelines.

572266

## 1 Introduction

This report reviews a failure analysis that was conducted for a power plant unit in Northern Greece. A failure had occurred in one of the power plant's heat exchange assemblies and more precisely, in one of the steam pipes. A high pressured and high-temperature steam pipe had ruptured causing a failure in the whole system.

The pipeline itself is 30 years old with regular maintenance. The author describes the pipe dimensions as 38 mm in outer diameter, wall thickness of 6 mm, and length of 4 meters. The pipe itself is made of at least two steel grades and joined together by welding. Materials are not known with certainty, but analysis points to

- 15Mo3,
- 13MoCr44, and
- 10CrMo910.

These are all common in production of pressure vessels. Pipeline had frequent maintenance that introduced downtime that increased operational costs.

## 2 Investigation methods and failure mechanisms

The author conducted several studies to analyse the failure. These included:

- macroscopic observations using stereomicroscopes,
- microscopic observations using scanning electron microscope that was equipped with an electron dispersive spectrometry X-ray microanalysis system for elemental analysis,
- metallographic examination of samples using inverted metallurgical microscope, and
- Vicker's hardness measurements using tester with a load of 10 kg.

The author also describes the preparation of samples using grinding, polishing, and etching with HNO<sub>3</sub> and ethanol solution.

The author considers four main elevated temperature failure mechanisms possible with that are:

- creep due to deviation between designed and actual operational parameters i.e., temperature and pressure,
- environmental factors, such as combustion gases and chemically introduced failure mechanisms,
- thermal fatigue due to frequent interruptions during maintenance, and
- high-temperature fatigue due to pressure fluctuations.

The designed operational parameters were relatively large compared to the actual operational parameters. Steam temperature in the inlet were designed to maintain at around 370 °C and outlet at 443 °C. The actual values were 449 °C at inlet and 505 °C at outlet. The author points out that the actual operational temperatures are in fact around 39.9 % and 43.0 % of the steel's melting point.

From macroscopic studies, the rupture itself is large and resembles a "fish mouth" thin-lip rupture that, according to the author, is common in creep-induced failure mechanisms with superheaters and reformer tubes. Wall thickness of the ruptured area had diminished from 6 mm

down to 1 mm. Wall thickness from the rupture tip to 120 mm further had worn from the original wall thickness of 6 mm to 4 mm (a reduction of 33 %).

From manufacturing point of view, the author claimed that the pipeline had occurring failures at curved areas of the pipe and near welded seams. Welded seams were analysed with more detail as in the failure analysis, the pipes consisted of two different steel grades: most likely 15Mo3 and either 13CrMo44 or 10CrMo910. The two different materials were welded together but microscopic analysis showed that there were no fusion zone or filler material being used. Hardness of the welded joint was tested, and the hardness increased with chrome-alloyed steel closer to the seam while hardness remained almost constant with low alloy steel (15Mo3). Scanning electron microscope was used to confirm recrystallisation of ferritic steel close to the welded seam. Nevertheless, the author concludes that the welded seam was an excellent quality as the rupture was clearly initiated from it.

The microscopic analyses showed an ununiform grain structure along the pipe. Using optical micrography, the author concluded that the grain structure of ferritic steel contained creep voids that eventually grew closer to the outer surface of the pipe. The re-crystallisation may have occurred due to high temperatures in welding process. The author points out that there are clear signs of cracks initiation near the weld seam and propagating almost along the pipe axis.

### 3 Failure analysis

The investigation conducted by the author strongly point towards multiple failure mechanisms. There is clear evidence of creep in the microscopic analyses. Presence of fatigue was most likely as the creep voids seem to have propagated cracks to the outer wall of the pipe. The primary cause of the failure is creep due to the mechanism in which creep void initiated crack propagation. Creep voids eventually combined and grew until cracks formed. Fatigue is even more likely as the author estimated that the overall stresses within the pipe were around 50.5 – 51.5 MPa and 15Mo3 has a fracture toughness of 56 – 95.7 MPa \*  $\sqrt{m}$  (Granta EduPack, 2023).

Granta EduPack (2023) defines maximum operation temperature for 15Mo3 as 538 °C and 13CrMo44 as 400 °C – 649 °C. The operational temperatures were relatively high compared to the melting temperature of the steel grades. This has most likely accelerated creep. Fatigue due to altering temperature and pressure in elevated temperatures are most likely the sources for stresses.

There are still other failure mechanisms that need to be addressed. Plastic deformation can be ruled out as there is clearly a rupture on the pipe while the pipe itself has not otherwise deformed. Plastic deformation could have happened if, for example, the pipe had collapsed by bending. Brittle fracture can be ruled out as the material itself was not brittle and not hardened in any way. Failure mechanisms that are due to chemicals can be ruled out as all introduced steel grades have either acceptable or excellent resistance to water and salt water.

For future operations, the author recommends the use of more heat-resistant steel grades and to reject the use of 15Mo3. This is most likely wise due to low maximum operation temperature and fracture toughness. Even though the introduced steel grades have good welding properties, post heat treating is highly recommended for more uniform crystal structure. With 15Mo3 and 13CrMo44, preheating and post weld heat treatments may be required (Granta EduPack, 2023). As there was a gap between the designed and actual operational parameters, designers of the system may have had selected other material for increased temperature and pressure.

100542646

## Materials safety: article exercise 2

This article contains a failure analysis for pipeline, which had a “fish-mouth” thin-lip rupture. The pipeline was used in high temperature and pressure conditions in a heat exchanger with steam running inside the tubes. Tubes were connected by welding. Material is not specified clearly, it is either 1.5415, 1.7335 or 1.7380 steel.

In this failure analysis, macroscopic observations were carried out using electron microscope (SEM), which was equipped with an electron dispersive spectrometry X-ray microanalysis system (EDAX). Metallographic examination was conducted using inverted metallurgical microscope. Cross-sections of the failed tubes were prepared by grinding and polishing. Chemical etching was also done.

Data recording showed that the damaged pipeline had failures occurring an average one per 15 days. This short lifetime of operation indicates about primary creep failure. These failures were investigated. Images show the fracture surface and cross-sections of inner/outer surface.

The primary cause for failure was creep. This can be seen in the cross-sections with voids initiation, voids growth and voids coalescence. The visco-plastic deformation caused by stress had caused intergranular creep by grain boundary sliding. The heat exchanger pipe system was designed to hold roughly 60-80 degrees less heat than was measured. General rule of thumb  $T(\text{melt})/2$  was still in place for the material, being 39-40% from melting point. Steam pressure was not able to be measured, which leaves greatly room for speculation. The cross section shows creep failure also by wall thinning on the other side of the pipe. Failure was located either at curved or close proximity to the circumferential weldments. There were no mention about the stress of the material and we do not know the effect of fatigue.

To prevent this failure in the future, more heat resistant material must be selected and complete re-design needs to be done.